# Stanford University 11th Annual Basin & Petroleum System Modeling Industrial Affiliates Meeting November 12-14, 2018

https://bpsm.stanford.edu/

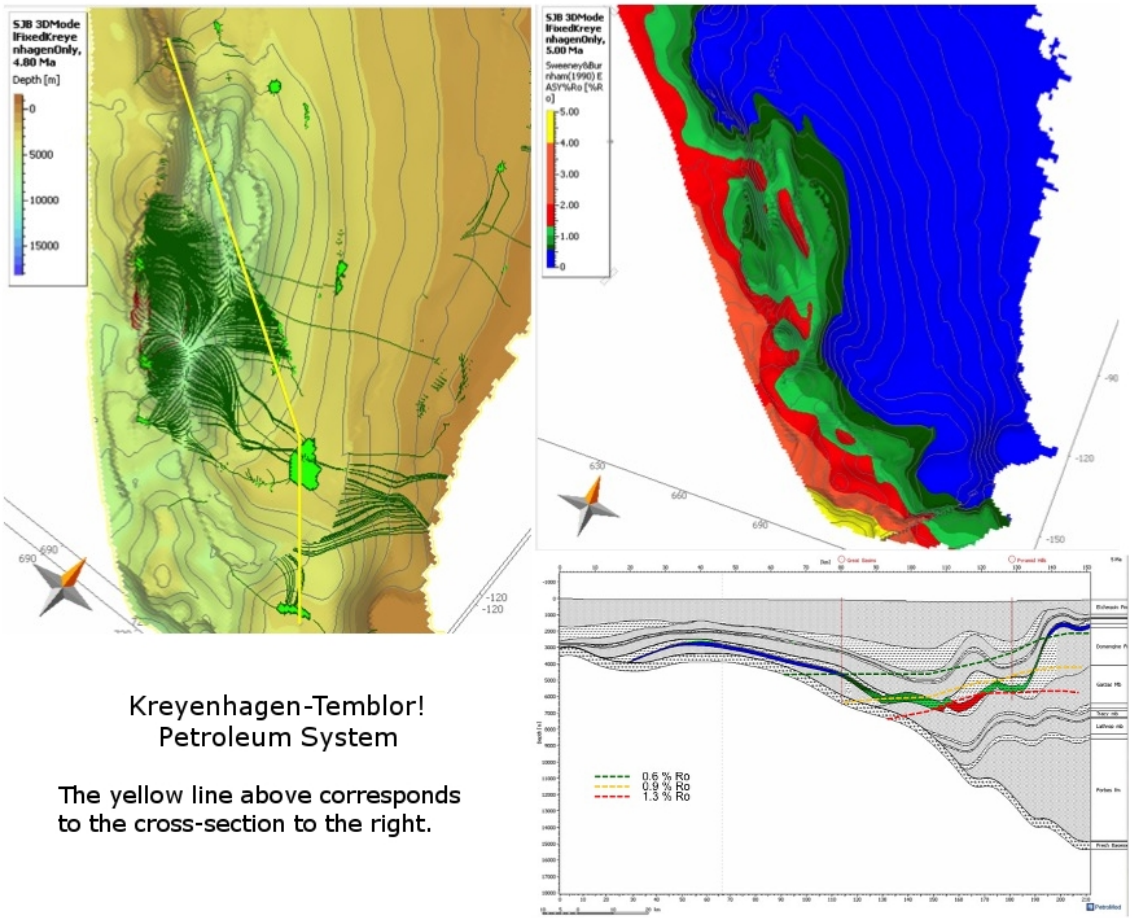


Kreyenhagen-Temblor! Petroleum System

The yellow line above corresponds to the cross-section to the right.

# Western San Joaquin Basin Field Trip & BPSM Oral Session

**Compiled by: S.A. Graham and L.B. Magoon**

*Harris Ranch Inn & Restaurant*
*Coalinga, California*

The eleventh annual Stanford University Basin and Petroleum System Modeling Industrial Affiliates Meeting is scheduled for Monday, Tuesday, and Wednesday, November 12-14, 2018. The conference will be held at Harris Ranch Inn and Restaurant in Coalinga, CA.

On Monday there will be an ice-breaker, hosted bar and hors d'oeuvres from 5:00 to 7:00 PM. Tuesday will be oral sessions by Stanford graduate students, who will present talks and be available for questions on their basin and petroleum system modeling research. Many of the principal advisors in the program will also be available for discussions.

Wednesday features a field trip to investigate the Kreyenhagen-Temblor(!) and essential elements of other petroleum systems in the western San Joaquin Basin, California. During the course of the day, we will be able to see all elements of that petroleum system, exposed due to geologically recent uplift/erosion.

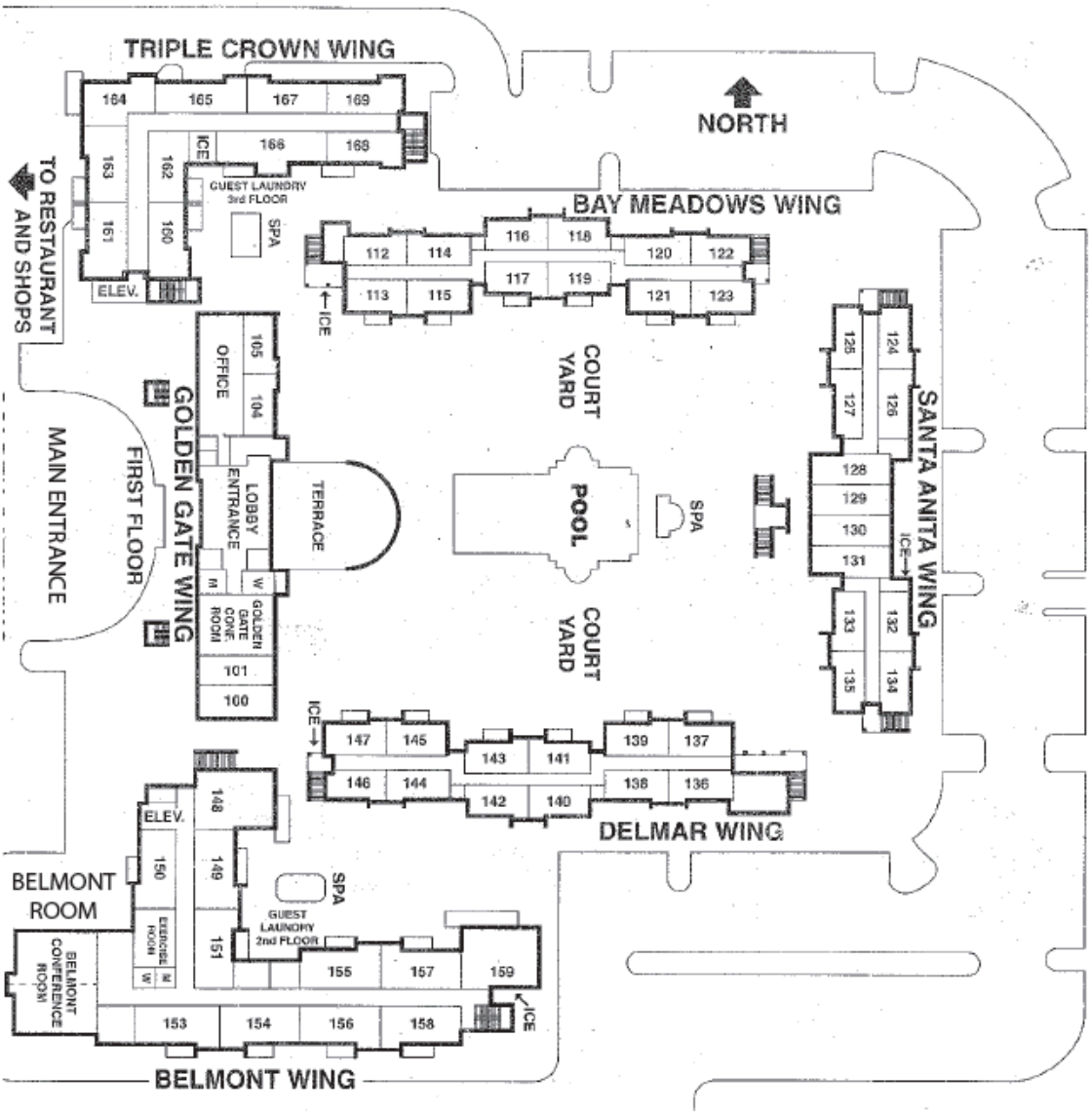


HARRIS RANCH
INN & RESTAURANT


## Meeting Attendees

| First | Last | Company | | First | Last | Company |
|---|---|---|---|---|---|---|
| Alexander | Hartwig | AkerBP | | Mustafa | Al Ibrahim | Stanford |
| Inessa | Yurchenko | BEG, UT-Austin | | Anatoly | Aseev | Stanford |
| Barbanti | Silvana | Biomarker Technologies | | Alan | Burnham | Stanford |
| Stephen | Palmes | BOEM | | Zachary | Burton | Stanford |
| Hui | Long | ConocoPhillips | | Laainam | Chaipornkaew | |
| Veit | Matt | ConocoPhillips | | Tanvi | Chheda | Stanford |
| Stoney | Clark | Equinor | | Laura | Dafov | Stanford |
| Greg | Jessome | Equinor Canada, Ltd. | | Stephan | Graham | Stanford |
| Stephen | Becker | ExxonMobil | | Xiaowei | Li | Stanford |
| David | Gombosi | ExxonMobil | | Leslie | Magoon | Stanford |
| Sabrina | Innocenti | ExxonMobil | | Mei | Mei | Stanford |
| Pedro | Miranda | Petrobas | | Tapan | Mukerji | Stanford |
| Anna | Svartman | Petrobas | | Leslie | Payne | Stanford |
| Kenneth | Peters | Schlumberger | | Anshuman | Pradhan | Stanford |
| Noelle | Schoellkopf | Schlumberger | | Marcelo | Silka | Stanford |
| Francois | Gelin | Total | | Pulkit | Singh | Stanford |
| Johannes | Wendebourg | Total | | William | Thompson-Butler | Stanford |
| Tom | Lorenson | USGS | | Qingwang | Yuan | Stanford |

# 11th Annual Stanford BPSM
# Industrial Affiliates Meeting
# November 13, 2018

| | |
|---|---|
| 8:30am | **Steve Graham,** Introduction |
| 8:50am | **Will Thompson-Butler**, Improved understanding of petroleum charge and migration in the middle Magdalena Valley, Colombia |
| 9:20am | **Zack Burton**, Basin and petroleum system modeling to test tectonic uplift as a mechanism for destabilization of gas hydrate |
| 9:40am | **Inessa Yurchenko**, The Cenomanian-Turonian Oceanic Anoxic Event (OAE2): Implications for source rock geochemistry |
| 10:00am | **Coffee Break** |
| 10:20am | **Silvana Barbanti**, Diamondoids: a revolutionary advancement in basin analysis and basin modeling |
| 10:50am | **Laura Dafov**, exploration and prediction of methane hydrates using basin and petroleum system modeling in northwest Walker Ridge, Gulf of Mexico |
| 11:20am | **Zack Burton**, New Zealand oil seep geochemistry: Insights into source rock depositional environment and age, source rock maturity, oil-to-gas cracking, and petroleum mixing |
| 11:40am | **Tanvi Chheda**, Constraining uncertainty in basin modeling of Jeanne d'Arc basin using measured data in Bayesian networks |
| 12:10pm | **Mei Mei**, Overview of Total-BPSM project on Petroleum Expulsion from Vaca Muerta Source Rock in Neuquén Basin, Argentina |
| 12:30pm | **Lunch** |
| 1:30pm | **Mustafa Al Ibrahim**, Geochemical properties of organic rich mudrocks using quantitative seismic interpretation |
| 1:50pm | **Anshuman Pradhan**, Integrating basin modeling and seismic imaging for uncertainty reduction |
| 2:20pm | **Laainam (Best) Chaipornkaew**, Basin-scale inelastic deformation of seal and source rock and its impact on overpressure prediction |
| 2:50pm | **Anatoly Aseev**, Fault sealing in oil and gas exploration: Existing methods and research motivation |
| 3:20pm | **Mei Mei**, Scientific underpinning of concepts of geochemical inversion: developing and improving methods with application to petroleum system analysis |
| 3:40pm | **Coffee Break** |
| 4:00pm | **Jon Payne**, Introduction to the modeling of carbonate depositional systems |
| 4:15pm | **Pulkit Singh**, Analytical equations for the growth of carbonate platforms |
| 4:40pm | **Xiaowei Li**, Interactions between sediment production and transport in the development of carbonate platforms: a case study from the Great Bank of Guizhou, China |
| 5:05pm | **Qingwang (Kevin) Yuan**, Scaling analysis of the coupled compaction, kerogen conversion, and petroleum expulsion during geologic maturation |
| 5:25pm | **Marcelo Silka**, Introduction and research interests |
| 5:35pm | **Les Magoon**, Introduction to petroleum system field trip |
| 6:00pm | **Adjourn**; reminder about group dinner |

# IMPROVED UNDERSTANDING OF PETROLEUM CHARGE AND MIGRATION IN THE MIDDLE MAGDALENA VALLEY, COLOMBIA

**William Thompson-Butler[1*], Kenneth E. Peters[1,2], J. Michael Moldowan[3], Leslie B. Magoon[1], Allegra Hosford Scheirer[1], Vladimir Orlando Blanco[4], and Roman Eugenio Gonzalez[5]**

[1]*Department of Geological Sciences, Stanford University, CA 94305*
[2]*Schlumberger, Mill Valley, CA, 94941*
[3]*Biomarker Technologies, Inc., Rohnert Park, CA, 94928*
[4]*Instituto Colombiano del Petroleo, Ecopetrol, Bucaramanga, Colombia*
[5]*Ecopetrol, Bogotá, Colombia*
[*]*rthomps@stanford.edu*

## Introduction

The Middle Magdalena Valley (MMV) is an intermontane basin and petroleum province in northwestern Colombia that, along with the Eastern Cordillera and Llanos, has acted as a regional sedimentary basin from the Triassic well into the Late Neogene (**Figure 1**). During the Cretaceous, restricted marine conditions within a broad foreland basin resulted mainly in the deposition of organic-rich carbonate and siliciclastic sediments in the area of the modern MMV (Cooper et al., 1995). While the Upper Cretaceous La Luna Formation is the primary regional source rock, the Cretaceous Tablazo and Umir Formations may also contribute (Zumberge, 1984; Ramon and Dzou, 1999). Despite over a century of petroleum exploration and multiple commercial discoveries (**Figure 1**), the complex burial and variable exhumation history associated with the Andean orogeny add uncertainty to the evaluation of petroleum systems in the MMV by impacting the distribution, quality, and thermal maturity of the Cretaceous succession of organic-rich source rocks. This study utilizes multivariate statistical analysis of source-related biomarker and isotopic ratios from oil samples to establish distinct oil 'tribes' and to infer differences in source rock depositional environment, lithology, and thermal maturity between them. Finally, vitrinite reflectance and Rock Eval data along with apatite fission-track data from published studies (i.e., Gomez et al., 2005) enable the construction of 1D models across the basin. These models illustrate the variable burial history and the impact on oil tribe distribution within the MMV.

## Summary and Conclusions

Hierarchical cluster analysis of 73 oil samples (**Figure 2**) defines six geochemically distinct oil tribes that may originate from different source rocks or from organofacies of the same source rock within the MMV (Peters et al., 2007). The tribes in this study show systematic distribution by both map location (**Figure 3**) and reservoir age. Tribes 1 through 4 are likely related to the primary regional source rock, the La Luna Formation. However, biomarker ratios (Peters et al., 2005) and alternating least squares analysis are used to observe regional differences in character and thermal maturity of the La Luna oil as well as mixing. The northernmost tribe in the MMV, Tribe 5, likely originates from the middle Cretaceous Tablazo or Rosablanca Formations. Tribe 6, in the southern MMV, is

the sole terrigenous oil identified in the study (Sofer, 1984), suggesting a non-marine source in the western flank of the Eastern Cordillera or an extension of the Cretaceous Umir Formation. Finally, diamondoid analysis shows the presence of secondary cracking in the Tribe 6 oil, while also suggesting input from a deeply buried and cracked source in the central MMV that may be the middle Cretaceous Tablazo Formation (Dahl et al., 1999).

While 6 tribes have been identified, more than half of the oil recovered in the Middle Magdalena Valley has come from a series of Tribe 1 fields in the central portion of the study area. In the area of these fields the total vertical depth subsea to the top of the Cretaceous interval ranges dramatically from less than 2,500 feet to greater than 10,000 feet (**Figure 4**). This disparity illustrates the lateral heterogeneity in both exhumation and modern day source rock burial depth. 1-D modeling can effectively illustrate the differences in burial history between the Norean-1 well in the northern MMV and the Cocuyo-1 well from the modern basin depocenter in the central MMV (**Figure 5**) and help put the variations found between petroleum tribes into the context of the local geologic history. However, to accurately characterize both charge timing and the presence of an early Cretaceous source suggested by diamondoid analysis, a full 2D model and structural restoration will be utilized.

**Figures**

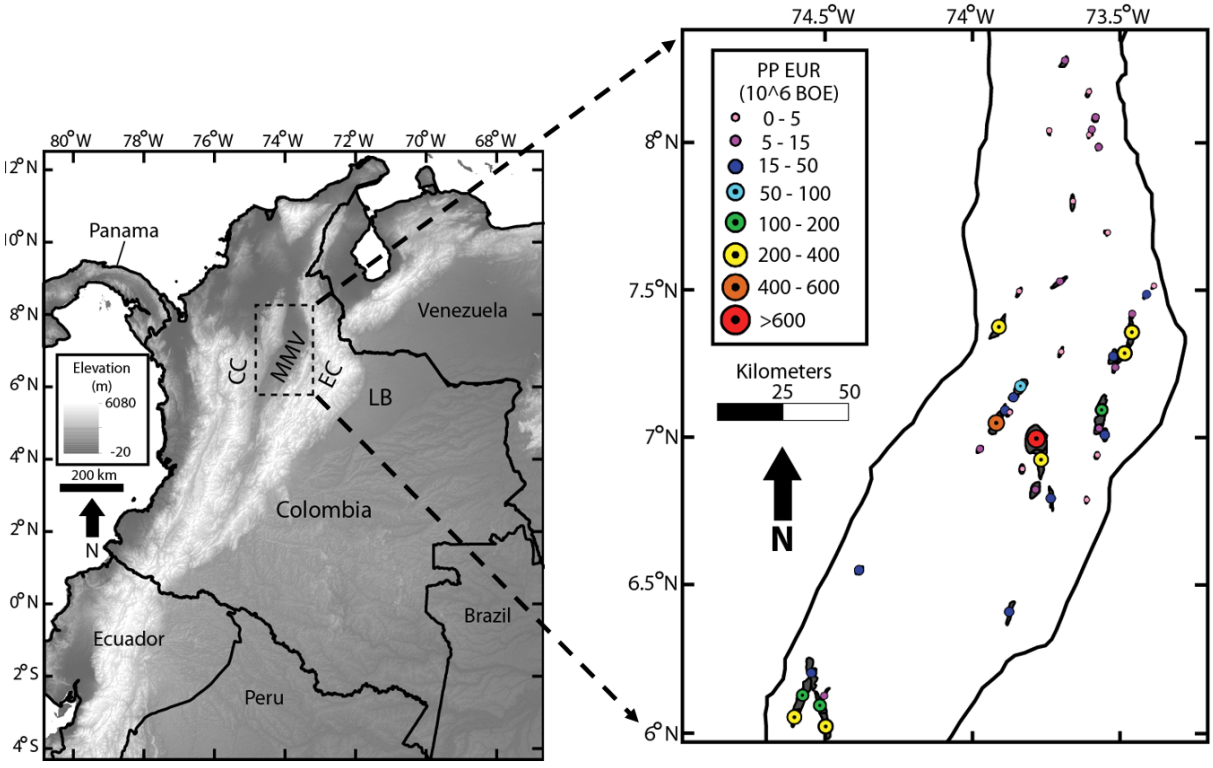


**Figure 1.** Map of Colombia showing elevation as well as the location of the Middle Magdalena Valley (MMV), Central Cordillera (CC), Eastern Cordillera (EC), and Llanos Basin (LB). Dashed box indicates location of Middle Magdalena Valley map used in

Figures 3 and 4. The inset box on the right gives the location and size of major oil and gas fields within the MMV in 10^6 proven probable estimated ultimate recoverable barrels of oil equivalent.

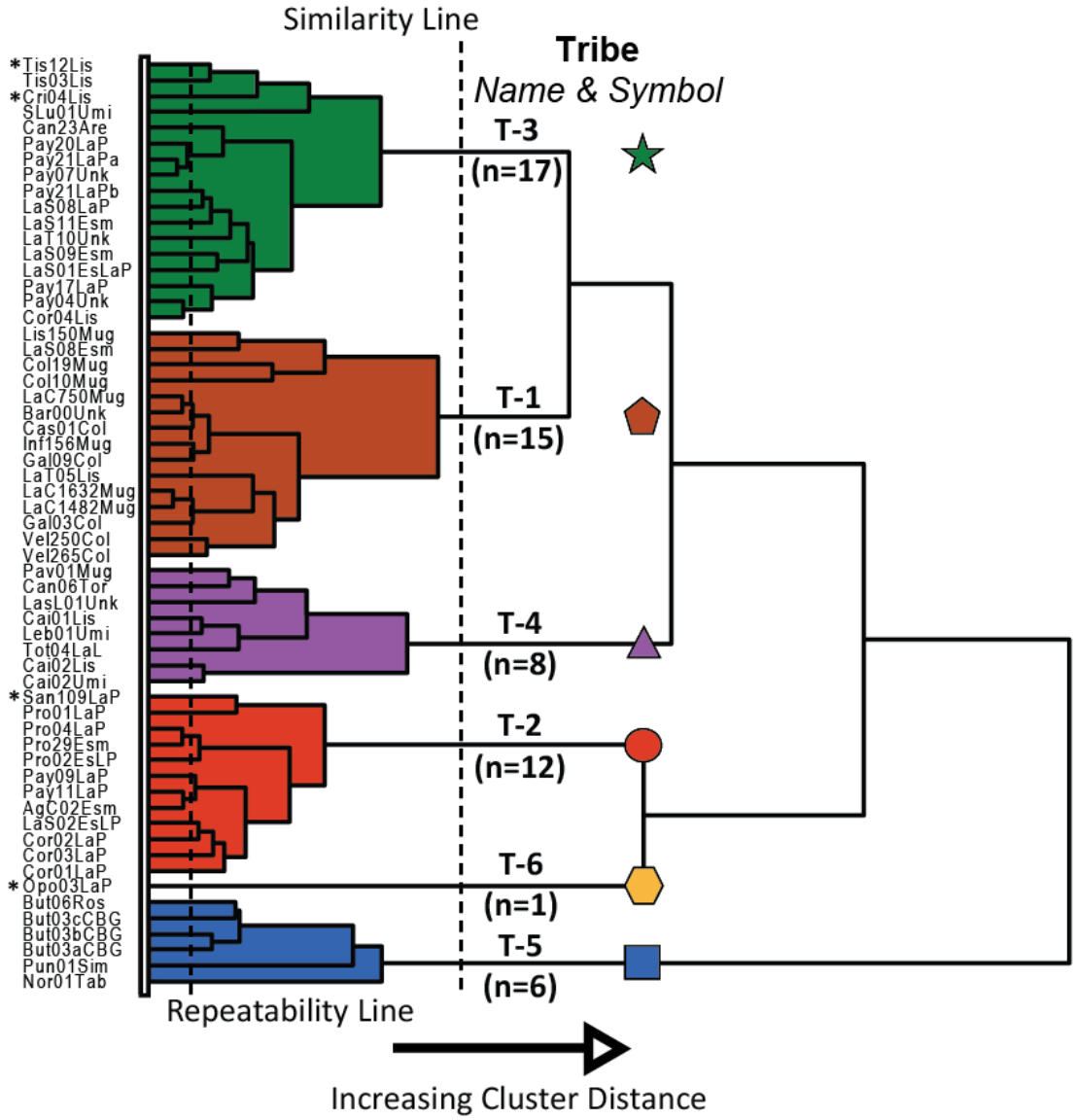


**Figure 2.** Hierarchical cluster analysis (HCA) dendrogram for the oil database provided by GeoMark Research. The HCA was built using 20 biomarker and isotopic ratios and identifies six total tribes in the Middle Magdalena Valley with the name, number of samples and map symbology for each tribe given. Samples marked by an asterisk were processed by both BTI and GeoMark Research. The Repeatability Line is based on the Pay20LaP and Pay21LaPa samples in Tribe 3 and the Pay09LaP and Pay11LaP samples in Tribe 2.

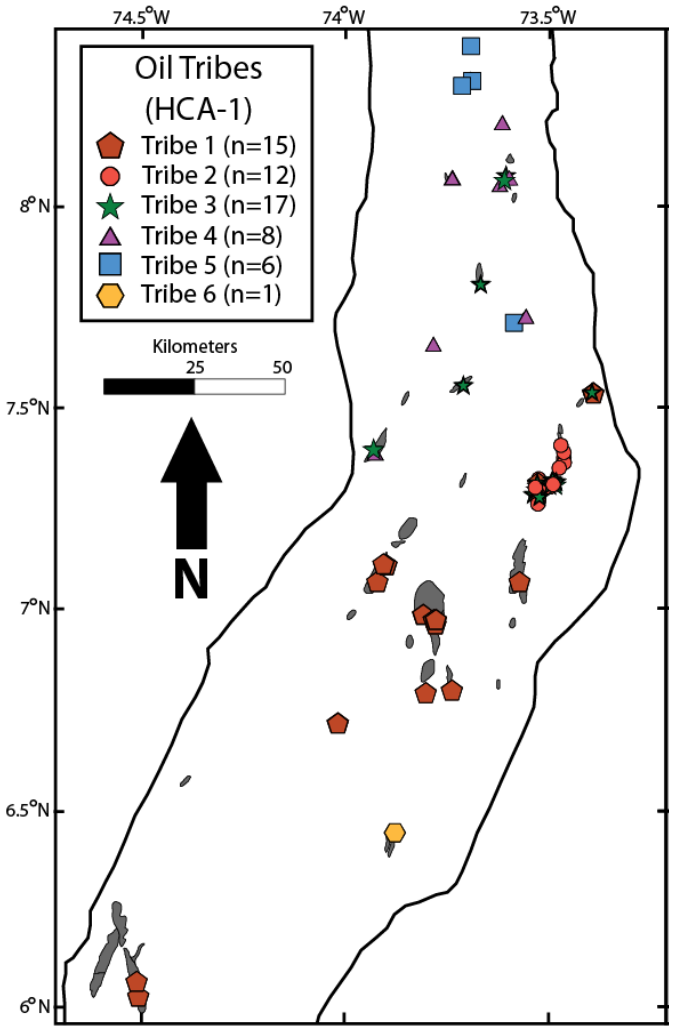


**Figure 3.** Map of the Middle Magdalena Valley showing the locations of oil samples used in HCA-1 with symbols indicating the petroleum tribe of each sample. Grey polygons are the locations of the primary oil fields in the MMV. Location of study area is indicated in Figure 1 by the dashed box.

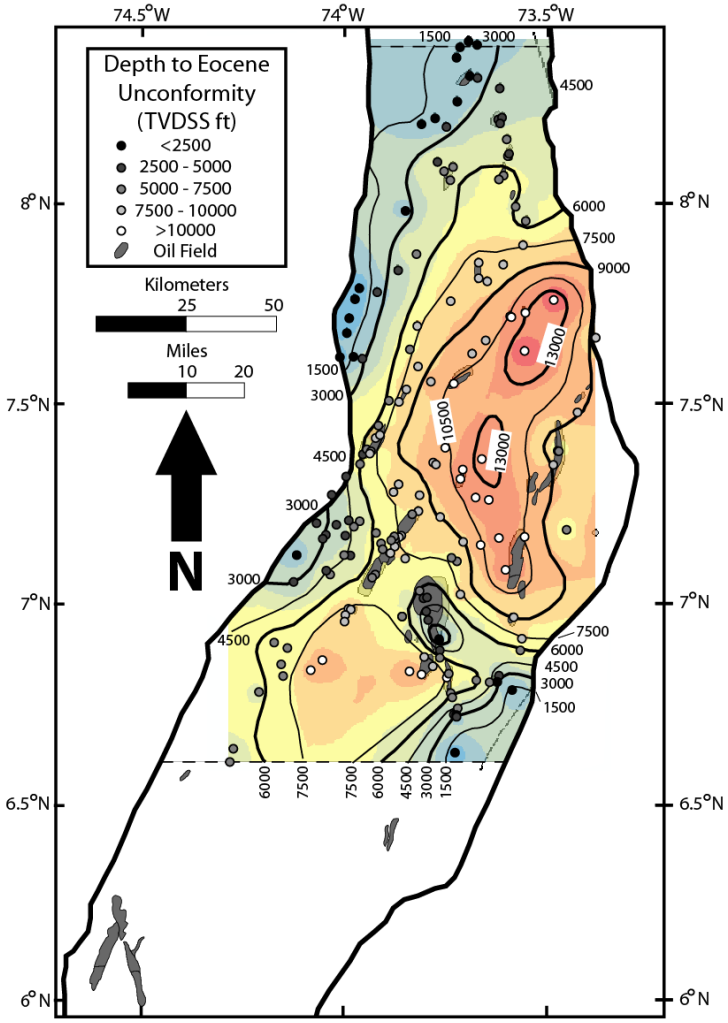


**Figure 4.** Map of the Middle Magdalena Valley contouring the depth to the top of the Cretaceous source rock package, marked by the Eocene unconformity, in total vertical depth subsea from 140+ wells. General deepening trends from both North to South and West to East exist in the MMV. Location of study area is indicated in Figure 1 by the dashed box.

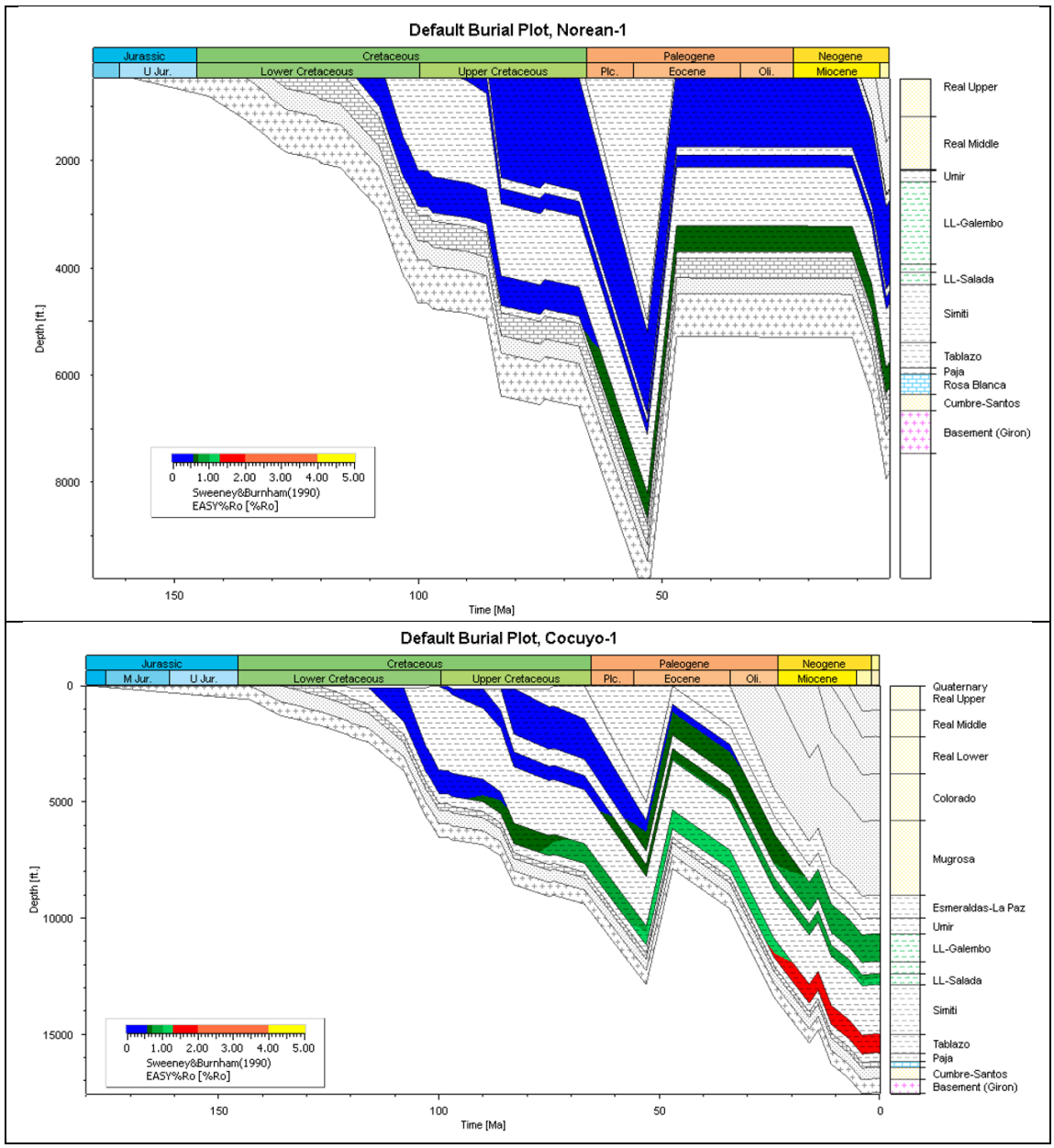


**Figure 5.** 1D modeling burial history results for the northern Norean-1 (above) and central Cocuyo-1 (below) wells within the MMV. Models are built from vitrinite reflectance, Rock Eval and formation top data from published sources as well as data shared by Ecopetrol for this study. The Galembo and Salada members of the La Luna Formation as well as the Tablazo Formation have a colored overlay reflecting the modeled vitrinite reflectance values for those units over time.


## Acknowledgements

The authors would like to thank Ecopetrol, GeoMark Research, and Petroleum Systems International (PSI) for providing oil samples and analyses for this study and for permission to publish this work. Special thanks go out to Biomarker Technologies, Inc., Infometrix, and the members of the Basin and Petroleum System Modeling Group at Stanford for many rounds of constructive review over the course of this project.

**References**

Cooper, M. A., F. T. Addison, R. Alvarez, M. Coral, R. H. Graham, A. B. Hayward, S. Howe, J. Martinez, J. Naar, R. Penas, A. J. Pulham, and A. Taborda, 1995, Basin development and tectonic history of the Llanos Basin, Eastern Cordillera and Middle Magdalena Valley, Colombia: AAPG Bulletin, v. 79, p. 1421-1443.

Dahl, J. E., J. M. Moldowan, K. E. Peters, G. E. Claypool, M. A. Rooney, G. E. Michael, M. R. Mello, and L. Kohnen, 1999, Diamondoid hydrocarbons as indicators of natural oil cracking: Nature, v. 399, p. 54-57.

Gomez, E., T. E. Jordan, R. W. Allmendinger, K. Hegarty, and S. Kelley, 2005, Syntectonic Cenozoic sedimentation in the northern middle Magdalena Valley Basin of Colombia and implications for exhumation of the Northern Andes: GSA Bulletin, v. 117, no. 5/6, p. 547-569.

Peters, K. E., L. S. Ramos, J. E. Zumberge, Z. C. Valin, C. R. Scotese, and D. L. Gautier, 2007, Circum-Arctic petroleum systems identified using decision-tree chemometrics: AAPG Bulletin, v. 91, no. 6, p. 877-913.

Peters, K. E., C. C. Walters, and J. M. Moldowan, 2005, The biomarker guide: Cambridge, UK, Cambridge University Press, 1155 p.

Ramon, J. C., and L. I. Dzou, 1999, Petroleum geochemistry of the Middle Magdalena Valley: Colombia: Organic Geochemistry, v. 30, p. 249-266.

Sofer, Z., 1984, Stable carbon isotope compositions of crude oils: application to source depositional environments and petroleum alteration: AAPG Bulletin, v. 68, no. 1, p. 31-49.

Zumberge, J. E., 1984, Source rocks of the La Luna Formation (Upper Cretaceous) in the middle Magdalena Valley, Colombia: Petroleum Geochemistry and Source Rock Potential of Carbonate Rocks (Palacas J. C., ed.), AAPG Studies in Geology #18, p. 127-133.

# BASIN AND PETROLEUM SYSTEM MODELING TO TEST TECTONIC UPLIFT AS A MECHANISM FOR DESTABILIZATION OF GAS HYDRATE

**Zachary F.M. Burton[1*], Allegra Hosford Scheirer[1], Yongkoo Seol[2], and Stephan A. Graham[1]**
[1]*Department of Geological Sciences, Stanford University*
[2]*U.S. Department of Energy National Energy Technology Laboratory*
**zburton@stanford.edu*

## Abstract
(*to be presented at AGU 2018; in preparation for publication*)

Gas hydrates form vast stores of greenhouse gas in deep-water marine sediment. Destabilization of gas hydrates has been suggested as a driver behind a greenhouse gas feedback effect, whereby methane released to the atmosphere leads to global warming. This warming could in turn lead to further destabilization of gas hydrates. Rising ocean temperatures and falling sea level are most commonly invoked as mechanisms behind methane hydrate destabilization, though recently tectonic uplift has also been suggested as a mechanism. However, the effect of uplift has not yet been modeled computationally.

## Methodology and results

Here, we utilize an East Coast Basin, New Zealand model based on previous structural restorations of the 124-kilometer Hawke's Bay CM05-01 seismic line (Burgreen-Chan et al., 2016). We simulate gas hydrate stability zone presence at various time steps, starting at 24 Ma. At 24 Ma, the East Coast Basin was at the end of a prolonged period of passive margin sedimentation. At 13.6 Ma, the basin was characterized by faulting and shortening, but not destabilization of gas hydrate. At 8.5 Ma, the basin was still characterized by faulting and shortening, but also by the onset of gas hydrate destabilization. At 7 Ma, the basin was characterized by the most extreme faulting and shortening, and by extensive and widespread disruption of the gas hydrate stability zone. Finally, at 0 Ma (Present Day), the basin is characterized by increased uplift and the persistence of just two isolated patches of gas hydrate stability zone in less than 10-kilometer-wide regions.

## Conclusions

Water depths greater than 500 meters between 24 Ma and 13.6 Ma are inferred to be the primary driver for preservation of the gas hydrate stability zone, whereas shallower depths significantly lower hydrostatic pressures causing extensive destabilization of the gas hydrate stability zone from 8.5 Ma to present (e.g., Handa, 1990). Our model results support the mechanism of tectonic uplift as a driver for large-scale methane hydrate destabilization. We suggest that uplift in the marine realm should be considered as a potential driver behind global climate change.

## References

Burgreen□Chan, B., Meisling, K.E. and Graham, S., 2016. Basin and petroleum system modelling of the East Coast basin, New Zealand: a test of overpressure scenarios in a convergent margin. *Basin Research*, 28(4), pp. 536-567.

Handa, Y.P., 1990. Effect of hydrostatic pressure and salinity on the stability of gas hydrates. *Journal of Physical Chemistry*, 94(6), pp. 2652-2657.

**Figures**

Figure 1. Map of New Zealand's North Island, indicating location of the East Coast Basin inboard of the subduction margin (bold black line with arrows); dotted line indicates the inboard/landward extent of the East Coast Basin; bold dashed line indicates location of the CM05-01 seismic line and the location of the model in Figure 2 and discussed in this study.

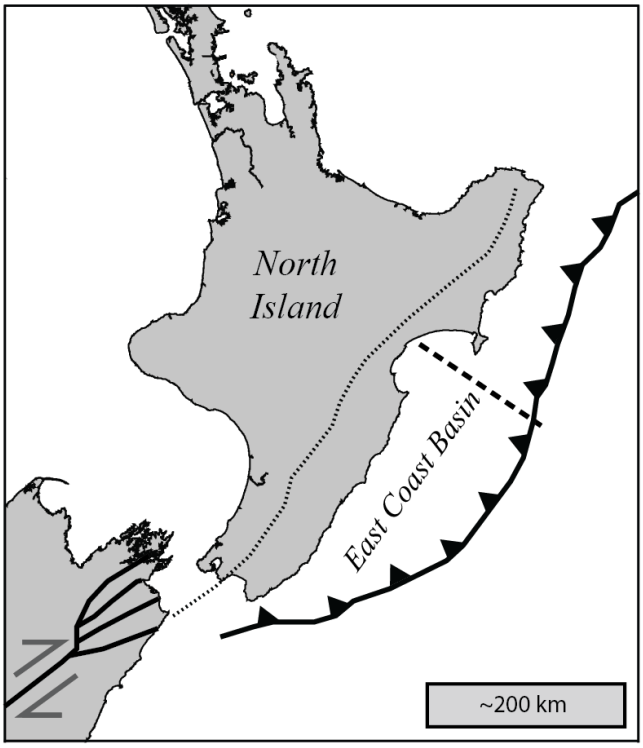


Figure 2. Model output for five timesteps; red coloring indicates the modeled location of the gas hydrate stability zone.

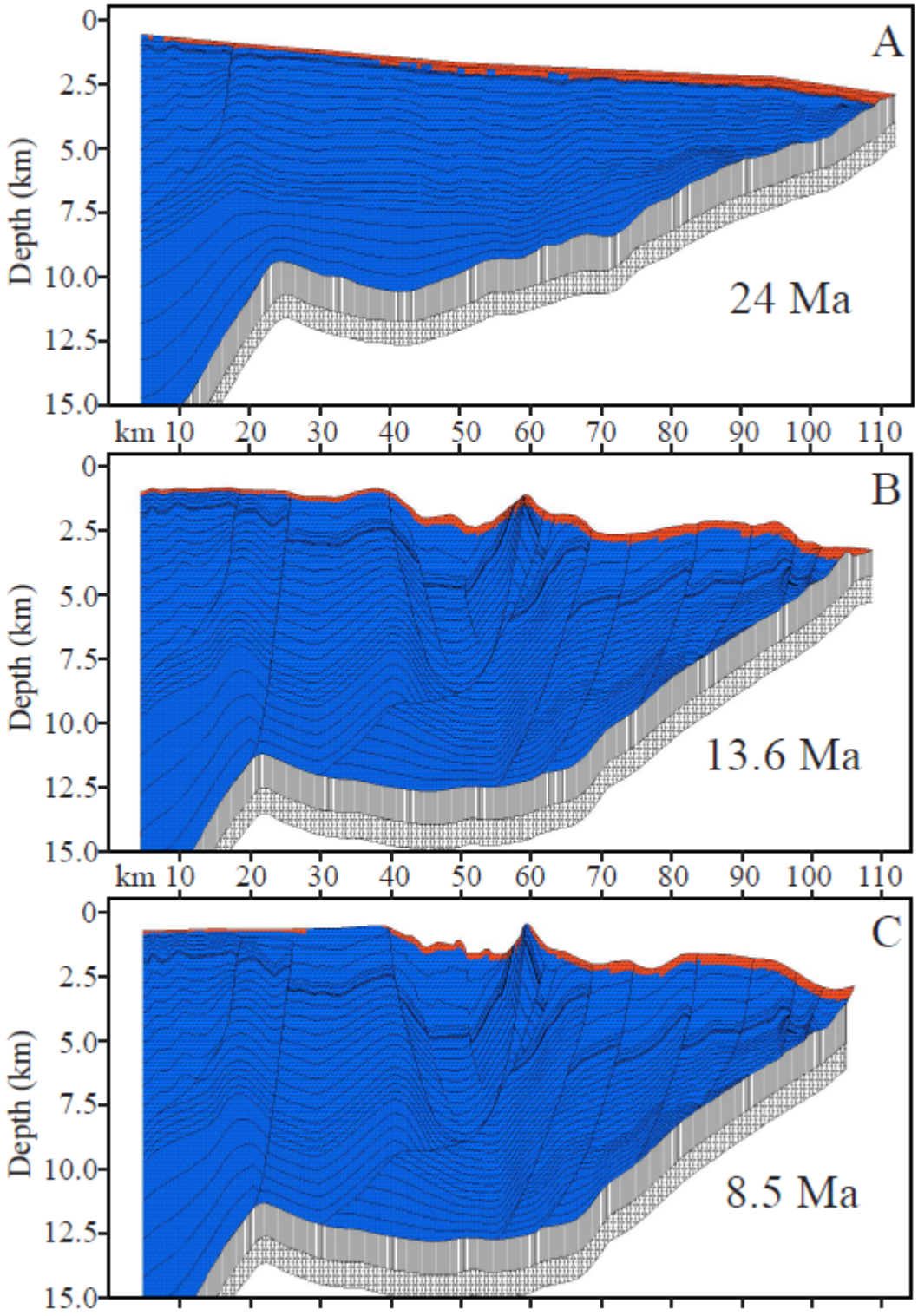
A
24 Ma
B
13.6 Ma
C
8.5 Ma
Depth (km)
0
2.5
5.0
7.5
10.0
12.5
15.0
km 10 20 30 40 50 60 70 80 90 100 110

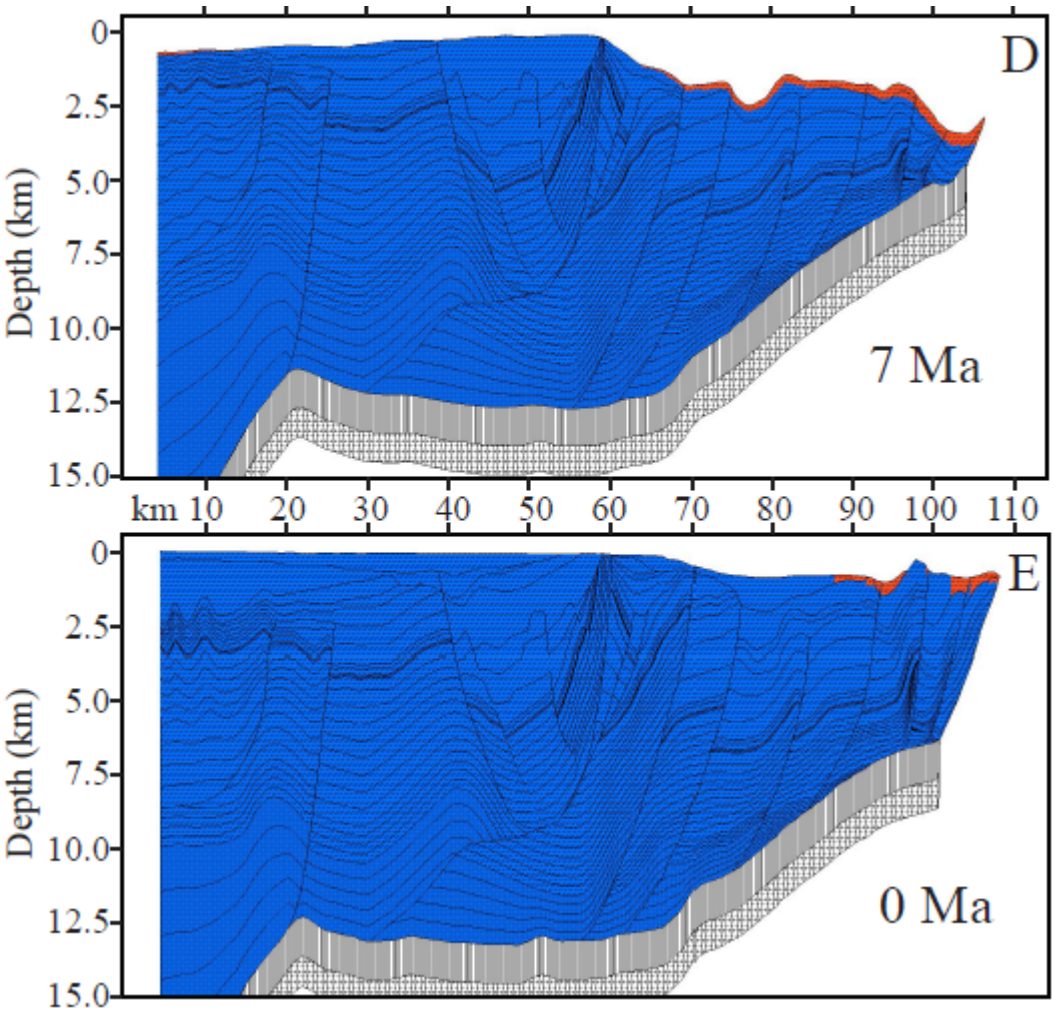
D
7 Ma
E
0 Ma
Depth (km)
0
2.5
5.0
7.5
10.0
12.5
15.0
km 10 20 30 40 50 60 70 80 90 100 110

# THE CENOMANIAN-TURONIAN OCEANIC ANOXIC EVENT (OAE2): IMPLICATIONS FOR SOURCE ROCK GEOCHEMISTRY

**Inessa Yurchenko[1,2], Mike Moldowan[3], Silvana Barbanti[3], Andrea Fildani[4], Rob Forkner[4], and Steve Graham[1]**
[1]*Department of Geological Sciences, Stanford University*
[2] *Bureau of Economic Geology, The University of Texas at Austin*
[3]*Biomarker Technologies, Inc.*
[4]*Equinor R&T*

## Abstract

The Cretaceous period (145−66 million years ago) encompasses important temporal and stratigraphic intervals for hydrocarbon source rocks deposition. It was characterized by a relatively warm climate, elevated atmospheric $CO_2$, and high eustatic sea levels. These conditions resulted in flooding of continental areas and creation of extensive shallow inland seas (e.g. Western Interior Seaway (WIS) in North America) favorable for organic-rich mudrock deposition worldwide (Eagle Ford, La Luna, Natih Formations to name a few). These Cretaceous world-class source rocks recorded climatic and paleoceanographic changes known as Oceanic Anoxic Events (OAEs) that are diagnostically expressed by widespread significant perturbation of the global carbon cycle. However, spatial and paleoenvironmental variability of OAE-related source rocks is understudied.

This work illustrates the preliminary results of postdoctoral research that centers on recording and understating geochemical (organic and inorganic) changes across the Cenomanian-Turonian OAE2 across the planet. We collected samples from Eagle Ford, Greenhorn, La Luna, and Bonarelli Formations to systematically record and understand the variability in biomarker, diamondoid, TOC, HI, $\delta^{13}C$, $\delta^{18}C$, iron speciation, and major and trace elements measurements that can occur within a single OAE-related event. In this presentation we focus on the USGS Portland-1 core (Greenhorn Formation near Cañon City, Colorado), which recorded key changes across the OAE2 interval, and analyzing key controls.

# DIAMONDOIDS: A REVOLUTIONARY ADVANCEMENT IN BASIN ANALYSIS AND BASIN MODELING

**J. M. Moldowan[1], J. E. Dahl[2], I. A. Yurchenko[3], and S. M. Barbanti[1]**
[1]*Biomarker Technologies, Inc., 638 Martin Avenue, Rohnert Park CA 94928.*
*jmmoldowan@biomarker-inc.com, sbarbanti@biomarker-inc.com*
[2]*Stanford Laboratory for Materials and Energy Science, Stanford University, Stanford, CA 94305.*
[3]*Bureau of Economic Geology, 10611 Exploration Way, Austin, TX 78758.*

## Introduction

The revolutionary technologies involving diamondoids include (1) quantitative diamondoid analysis (QDA) used for determining the extent of oil cracking and maturity of oil samples in both conventional and unconventional applications, and (2) quantitative extended diamondoid analysis (QEDA) to reveal and correlate the sources of oil samples. The application of diamondoid technologies to different geological areas, Santos Basin, Brazil, and North Slope, Alaska, is discussed in this work.

## Methodology and results

We applied the quantitative extended diamondoid analysis (QEDA) for pre- and post-salt sourced oil samples from Santos Basin in order to correlate them with the deep pre-salt sources represented by oil samples 16, 17 and 18 (Figure 1). The pre-salt oil samples display a nearly perfect correlation of their QEDA fingerprints and because the oils are not seen by QDA to be cracked, they serve as the QEDA trace of the pre-salt lacustrine source formation. Some highly cracked oils from post-salt reservoirs exhibit the same trend in QEDA indicating they were derived from lacustrine Lagoa Feia deep source rock. Some thermally cracked oil samples that have an overall marine oil biomarker signature show similar QEDA signature to that of pre-salt oils. This fact may imply that these oils are mixed from a marine source in the oil-window and a lacustrine source from deep (Figure 1).

## Summary and Conclusions

The occurrence of deep-sourced contributions and co-sourced mixtures is common in the Santos Basin demonstrated by the extent oil cracking plot based on QDA data. The deep sources are correlated by using QEDA and linked to source-rock families by end-member non-cracked, non-mixed oils. Three deep-sourced oil families, two marine and one lacustrine, have been indicated by using the QEDA diamondoid fingerprinting method.

## Figures

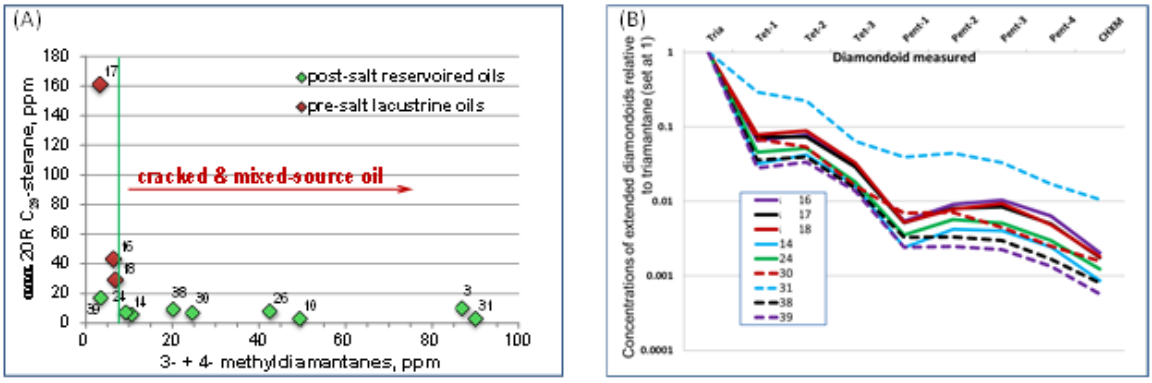


**Figure 1**. Diamondoid analyses reveal the extent oil cracking and determine affinities of deep sources in Santos Basin. (a) QDA shows most Santos Basin oils are mixtures from shallow and deep sources. The pre-salt oil samples show low diamondoid concentrations typical of oil window and non-cracked oil. (b) Extended-diamondoid fingerprints show three patterns in the oil set: pre-salt and related oils display one unique pattern, whereas oils with a marine source show two different patterns, which may be related to two distinct marine sources within the middle to upper Cretaceous sedimentary sequence.

## References

Barbanti, S.M., Moldowan, J.M., Dahl J.E., Bott, G., Tikaki, T., Moldowan, S.M., 2014. Advanced Geochemical Technologies for Determining Multiple Sources, Facies and Oil-Mixtures of Oil Produced in the Santos Basin, Brazil [abs.], in Proceedings of 14$^{th}$ALAGO, Armação dos Búzios, Brazil, OG21.

Yurchenko, I.A., Moldowan, J.M., Peters, K.E., Magoon, L.B. and Graham, S.A., 2018. Source rock heterogeneity and migrated hydrocarbons in the Triassic Shublik Formation and their implication for unconventional resource evaluation in Arctic Alaska. Marine and Petroleum Geology, 92, pp. 932-952.

Yurchenko, I.A., Moldowan, J.M., Peters, K.E., Magoon, L.B. and Graham, S.A., 2018. The role of calcareous and shaly source rocks in the composition of petroleum expelled from the Triassic Shublik Formation, Alaska North Slope. Organic Geochemistry, 122, pp. 52-67.

# EXPLORATION AND PREDICTION OF METHANE HYDRATES USING BASIN AND PETROLEUM SYSTEM MODELING IN NORTHWEST WALKER RIDGE, GULF OF MEXICO

**Laura Dafov[1], Allegra Hosford Scheirer[1], Oliver Schenk[2], Stephan Graham[1], Noelle Schoellkopf[3], and Yongkoo Seol[4].**
[1]*Department of Geological Sciences, Stanford University*
[2]*Schlumberger, Aachen, Germany*
[3]*Schlumberger, Danville, CA*
[4]*National Energy Technology Laboratory, Morgantown, WV*

## Introduction

Application of exploration methods to assess gas hydrates is recently expanding in the science community. One of the most comprehensive and integrated methods is basin and petroleum system modeling (BPSM), as a tool to estimate methane hydrates saturation, distribution, and volumes in place. We apply BPSM to 3D seismic and well log data in Walker Ridge block 313, using 3D modeling of the Terrebonne Basin and 2D model extraction to quickly answer questions, with interesting findings thus far.
Since 1985, five published hydrate in-place estimates were made of the Gulf of Mexico with large variation from ~800 to 45,000 tcfg (Boswell et al., 2012). BPSM integrates a large number of basin-scale and reservoir-scale inputs at fine spatial and time resolution (vertical cell thickness of 10cm and 100-year time steps) for an accurate prediction of the gas hydrate stability zone (GHSZ). 3D BPSM of Terrebonne Basin will allow for a better constrained hydrate in-place estimate.
Through modeling, we elucidate compaction and deformation through time due to hydrate saturations and whether lithology differences play a significant role in GHSZ thickness through time. Lastly, the ability of hydrates to sufficiently impact diagenesis critical to seal development and integrity is addressed.

## Methodology

We investigate the GHSZ in detail for the Pleistocene "orange sand" and other reservoir units in the Terrebonne Basin of the GOM using seismic data and well logs. The reservoir rocks are described by color nomenclature used in literature (e.g. Boswell et al., 2012). A gas (methane) hydrate reservoir is defined as pore-filling sandstone saturated by clathrate, or hydrate, at relatively higher saturation (>10%). We test hypotheses by using the interpretations to create a pseudo 2D and later a 3D integrated BPSM. Resistivity markedly increases at the hydrate saturated orange sand body. Resistivity log is one of several logs which are used to explore for and predict hydrate saturations. The orange sand experiences a polarity or phase reversal in the seismic at the base of the gas hydrate stability zone (BGHSZ) (Figure 1). This is a subtle direct hydrocarbon indicator of hydrate overlying a free gas reservoir.

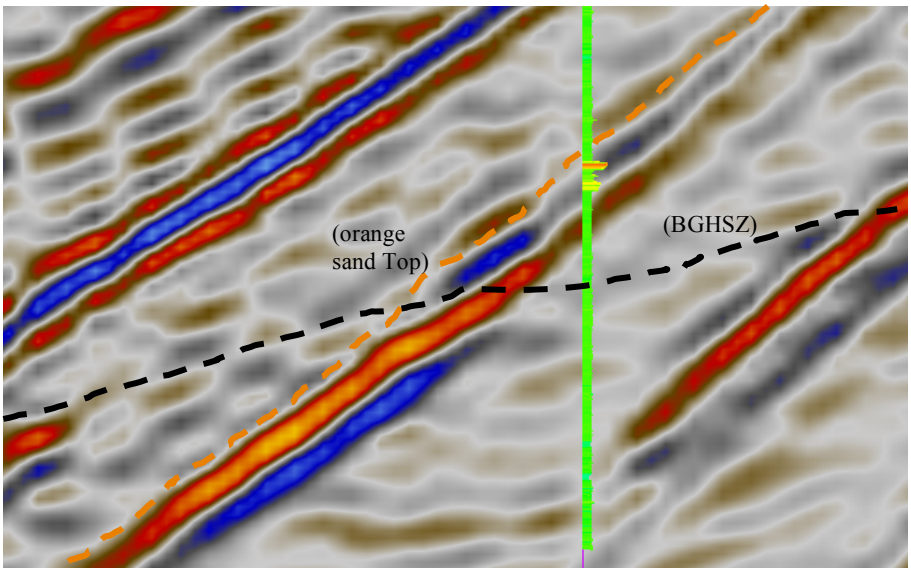


**Figure 1.** Polarity or phase reversal identified in "orange sand" of seismic interpretation, generally used as a method to map out base of GHSZ (BGHSZ) in the GOM and used to validate model output of BGHSZ. Well H resistivity curve overlain.

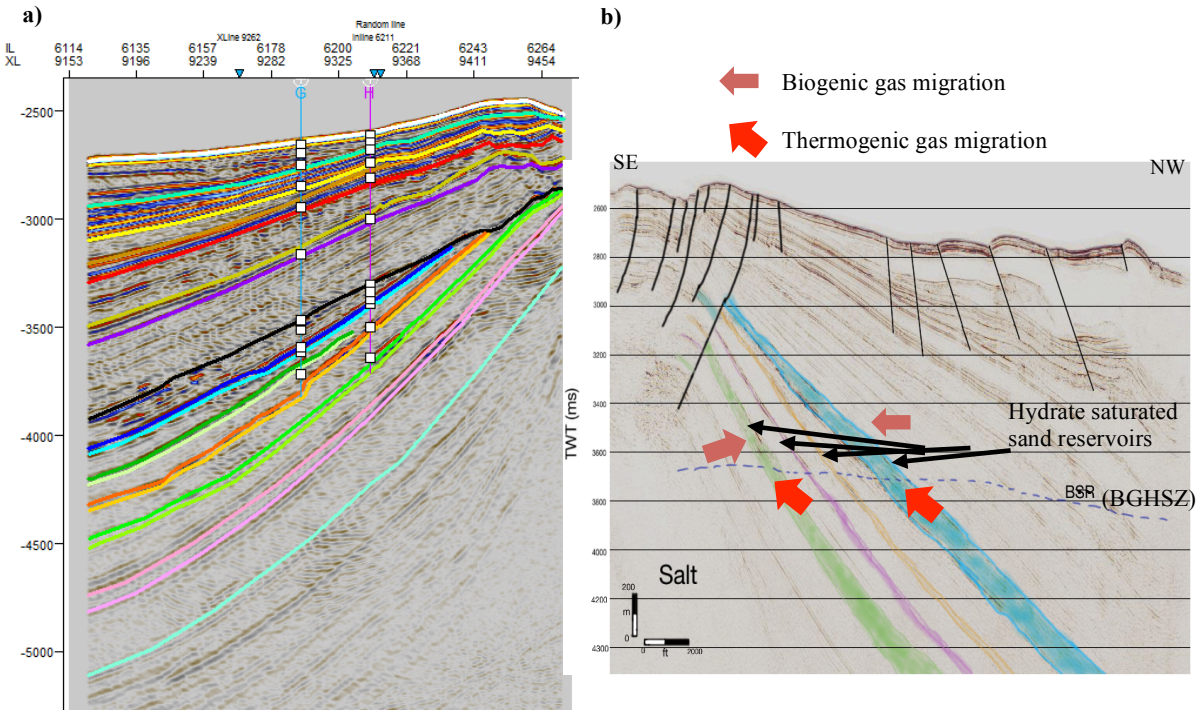


**Figure 2.** Interpreted seismic and well log horizons used for 3D model. a) Color convention of horizons based on literature nomenclature. Seismic horizons align well with picks from wells based on gamma ray and resistivity interpretations. VE x8. b) Hypothesized migration pathways, BGHSZ, and potential reservoirs with increased hydrate saturations.

2D seismic from the USGS was interpreted to hypothesize reservoirs (Figure 2b) and 3D seismic (Figure 2a) was used to pick 3D horizons for the 3D model geometry (Figure 3). The 2D model is a synthetic 2D model used as a case for controlled inputs with varying lithology input to test the hypothesis of effect of thermal conductivity on GHSZ. Input thicknesses of lithology are based on well data from Walker Ridge industry well WR313#001.

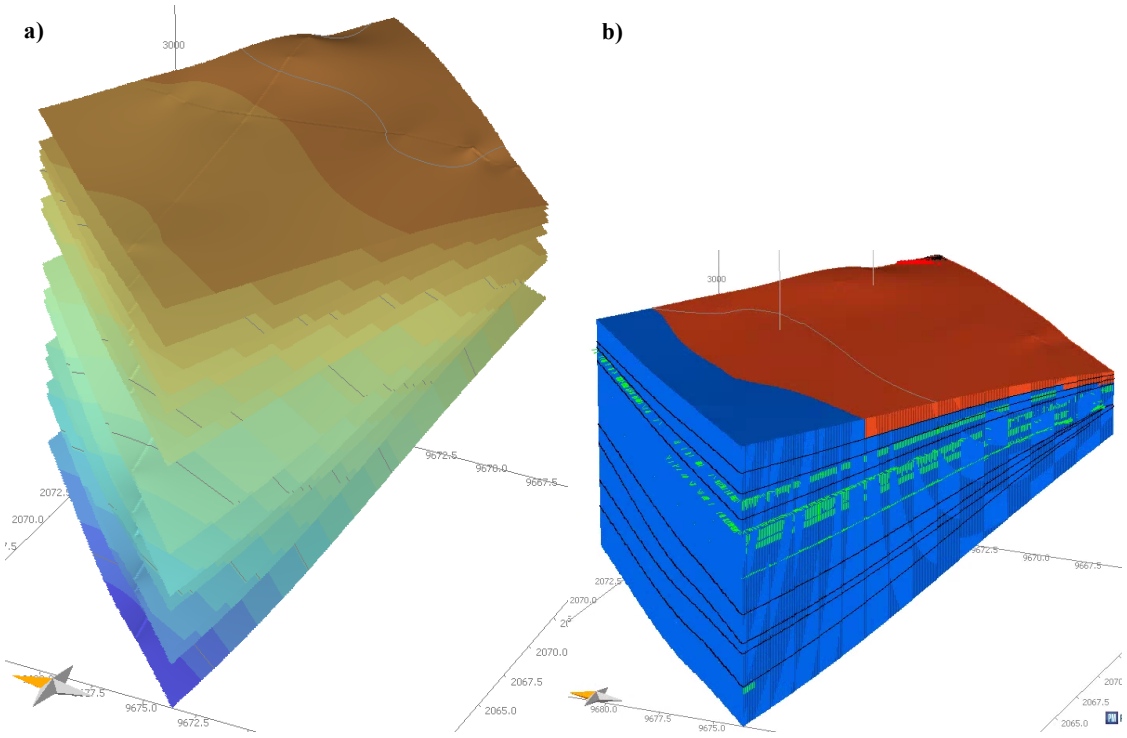


**Figure 3.** 3D model of Terrebonne Basin Walker Ridge block 313. a) Surface inputs, VE x8. b) simulated model with red as the gas hydrate stability zone. Green color is hydrocarbon migration vectors.

**Basin model and results**

The 3D model simulated the GHSZ on a large scale and the vertical resolution is low to allow for reasonable run time. In the future, layers will be split for higher resolution. This large-scale analysis showed generation and migration of thermogenic gas. To get a better understanding of details, such as thermal conductivities of detailed stratigraphy from well logs, we use the 2D model to investigate processes in more detail to validate hypotheses. Lithology variations not only impact thermal conductivity and thus the depth of GHSZ, but they also produce different compaction behavior. Compaction behavior is further altered by saturation of hydrates in pore-filling reservoirs (Figure 5).

The synthetic 2D non-dipping model (Figure 4) limits methane contribution to the GHSZ from biogenic gas generated and accumulated by short-distance migration. In the 3D model (Figure 3b), dipping sand beds are hypothesized to serve as conduits to long range

thermogenic methane migration. Notice the variable bathymetry (Figure 3) and at the large scale, the stratigraphic beds dipping due to a salt diapir; but at the smaller scale, local anticlines may have formed due to hydrates.

Figure 4 displays an inverse relationship between thermal conductivity of differing lithologies in deposition and GHSZ thickness through time- an important consideration for modeling hydrates. This finding seems intuitive, but, it was not addressed in recent hydrates modeling in any literature that first author has reviewed thus far. The range of GHSZ thickness due to changes in lithology tested in this model is 1,260 ft to 1,370 ft, or a difference of 110 ft column- a significant thickness when calculating gas volumes.

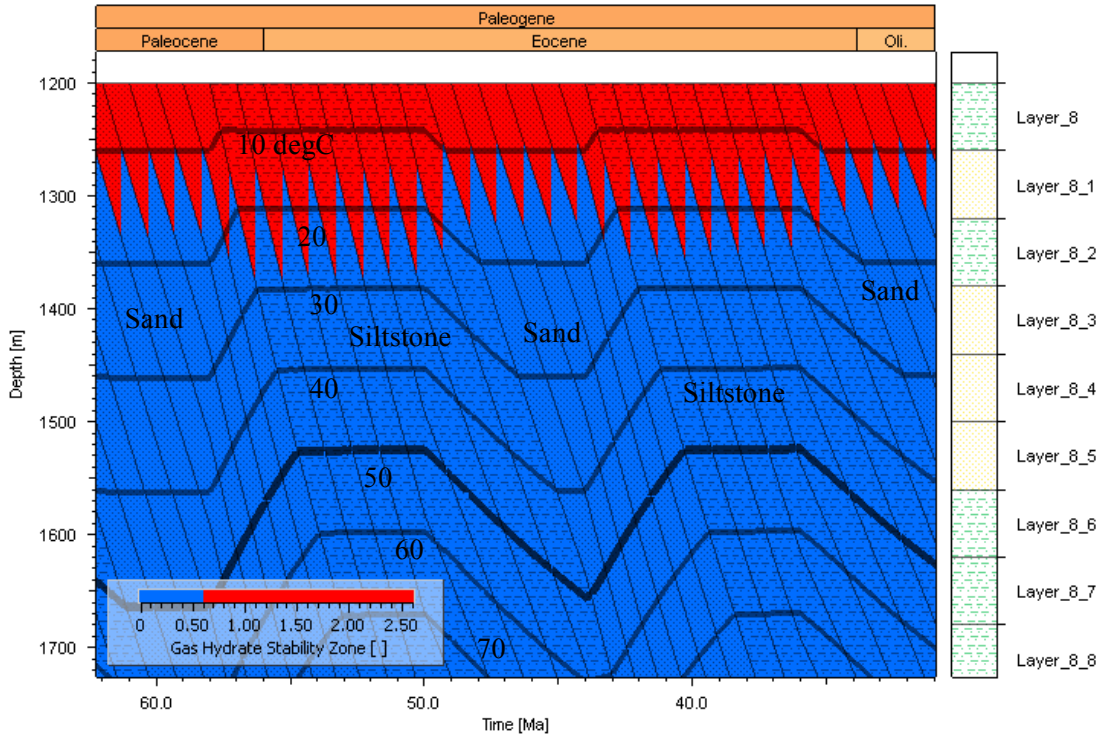


**Figure 4.** Burial diagram extracted from 2D model results. The inverse relationship between thermal conductivity of lithologies and GHSZ thickness. Sands indicates by dots, siltstone by dashed lines. GHSZ thickness through time in red. Temperature isolines in bold black lines.

Another interesting result of the extracted 2D model, is observed hydrate saturations (Figure 5). As hypothesized, the bottom third of the GHSZ contains thin sands which are relatively higher hydrate saturated (30-40%) than adjacent siltstone (0-25%). This is due to capillary pressure and preferred pressure-driven migration of methane. The upper two thirds of the GHSZ contains siltstone layers predicted to be saturated with hydrates as high as 100%, which are suspected to be sourced primarily by biogenic methane. The character of the host is suspected to be fracture filling based on literature. As the depth of the GHSZ shifts through time, it is hypothesized that the fracture-filling hydrates may dissociate and thus methane can migrate to neighboring sand deposits. Lastly,

compaction is inhibited because hydrate fills the pore space, which through time, may create local anticlines and force gas migration towards the local highs.

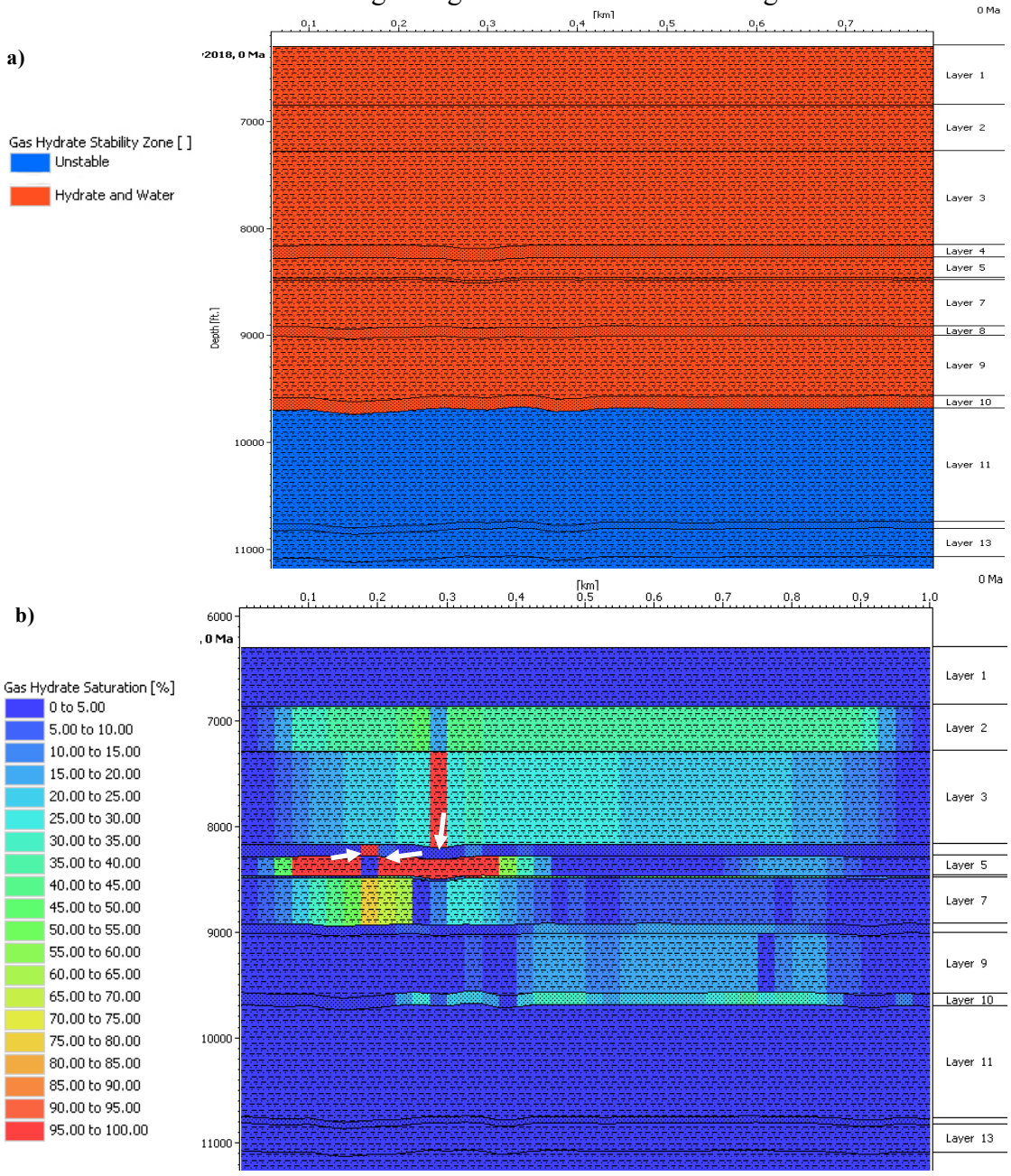

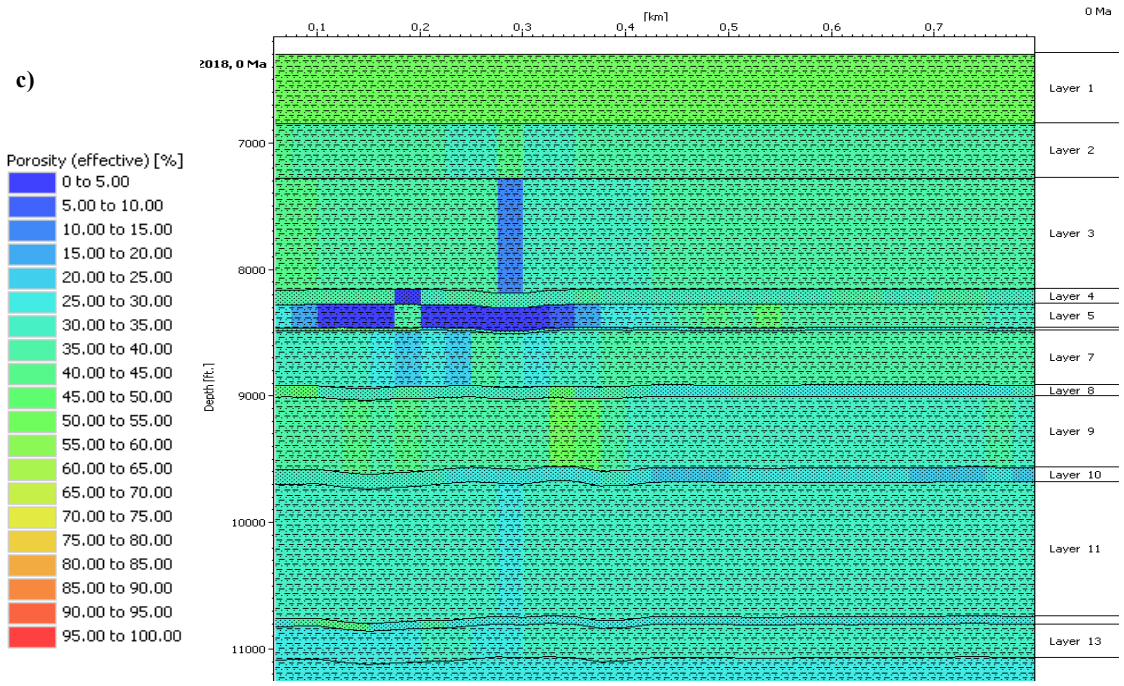


**Figure 5.** 2D "non-dipping" simulated model with a) GHSZ at present-day b) methane hydrate saturation variation throughout the GHSZ and c) effective porosity.

## Conclusions and Future Work

In summary, BPSM proves to be a fast and effective tool for estimation of hydrate saturations and for answering hydrates exploration questions. Type of lithology proves to be an important factor affecting basin temperature and hydrate stability zone thickness. Through time, diagenesis and structure are also affected by the formation and dissociation of hydrates. Soon, we will study in more detail the biogenic versus thermogenic methane contributions to the GHSZ.

Thanks to private correspondence with Robert Kaminsky, ExxonMobil Upstream Research Company, future model scenarios include testing hydrates as seals to answer the following questions: Can quantitative risk prediction be developed for predicting leakage occurrence through hydrates zones? Assess reservoir formation models and determine under what conditions can hydrates play a major trapping role given the temperature history and hydrate zone history? This test case has free gas beneath the hydrates, based on BSR in seismic and previous drilling results, so here the hydrates are an effective seal. A question to be explored is- what conditions allow hydrates to be an effective seal here and how can it vary based on different geologic variables?

## Reference

Boswell, R., Collett, T.S., Frye, M., Shedd, W., McConnell, D.R., and Shelander, 2012, Subsurface gas hydrates in the northern Gulf of Mexico, v. 34, i. 1, p. 4-30.

# NEW ZEALAND OIL SEEP GEOCHEMISTRY: INSIGHTS INTO SOURCE ROCK DEPOSITIONAL ENVIRONMENT AND AGE, SOURCE ROCK MATURITY, OIL-TO-GAS CRACKING, AND PETROLEUM MIXING

**Zachary F.M. Burton[1*], J. Michael Moldowan[1], Leslie B. Magoon[1], Richard Sykes[2], and Stephan A. Graham[1]**
[1]*Department of Geological Sciences, Stanford University*
[2]*GNS Science, New Zealand*
**zburton@stanford.edu*

**Abstract: Source rock depositional environment and age**
(*presented at AAPG 2018; submitted for publication*)

New Zealand's East Coast Basin contains over 300 oil and gas seeps and shows. Nonetheless, understanding of petroleum system characteristics (and in particular, source rock characteristics) remains quite limited. Geochemical characteristics of oil seeps are used to assess source rock properties in the East Coast Basin.

**Methodology and results**

Here, biomarker fingerprints of crude oil samples from four onshore East Coast Basin oil seeps were used to assess source rock characteristics including type of organic matter input, redox conditions, sedimentary facies, and age. Results show that samples generally form two groups, correlating with geographic location: a northern and a southern group. Source rocks associated with all seep samples are interpreted to be marine. However, results suggest northern samples had more terrigenous organic matter input to their source rock(s), while southern samples had more marine input. Results suggest northern sample source rock(s) had more oxic depositional environments, whereas southern sample source rock had more reducing environments. A shale source rock sedimentary facies was indicated for all samples. These observations suggest that southern samples may be derived from slightly higher quality source rocks (higher HI, deposited in more reducing conditions), although source rocks in both regions are oil prone. Biomarker age parameters suggest that the northern oil samples are from a younger (Cenozoic) source rock, whereas the southern oil samples are from an older (Cretaceous) source rock.

**Conclusions**

Source rock characteristics (depositional environment and age) point to the presence of two different source rocks. We postulate that northern oils samples from younger source rock with more terrigenous organic matter input represent the Late Paleocene Waipawa Formation, whereas southern oil samples from older source rock with more marine organic matter input represent the Upper Cretaceous to Paleocene Whangai Formation.
**Abstract: Source rock maturity, oil-to-gas cracking, and petroleum mixing**
(*published in Energy & Fuels, 2018*)

Determining oil quality is essential to identifying valuable resource accumulations. However, in new areas of exploration, little information is available on the processes affecting resource quality. Geochemical analyses of oil seeps from frontier regions of New Zealand's East Coast illustrate an application of underutilized resource quality assessment techniques, and provide an understanding of source rock maturity, oil quality, secondary cracking, and mixing of petroleum fluids.

**Methodology and results**

Analytical geochemical techniques are used to reveal oil seep characteristics. Analysis of *n*-alkane and isoprenoid distributions reveals biodegradation, and thus potentially lower oil quality in the southern versus the northern oil seeps. However, sterane and terpane compounds are unaltered, indicating overall biodegradation of these oils is low to moderate. Additionally, lack of 25-norhopane indicates degradation of southern oils may be solely aerobic. Therefore, any subsurface accumulations are potentially unaffected. Investigation of sterane and hopane isomerization ratios and additional sterane and terpane maturity parameters is paired with diamondoid analyses of oil-to-gas conversion and petroleum mixing. Three distinct petroleum mixtures are identified among the sampled seeps: (1) a seep composed of an early/peak oil window component and an intensely cracked condensate/wet gas component, (2) seeps solely containing a peak/late oil window component, and (3) a seep composed of a peak/late oil window component and an intensely cracked condensate/wet gas component.

**Conclusions**

Studied oils have been subjected to relatively low levels of biodegradation. The identification of petroleum mixtures and mixture components indicates at least three distinct charges or stages of petroleum generation. Black oil components might indicate actively producing source rock in all regions represented by the seeps. Intensely cracked components indicate petroleum mixing via thermogenic gas infiltration and suggest an effect on oil quality. Important questions concerning migration pathways and timing, ties to New Zealand's offshore basins, and potential for reservoir entrapment of these petroleum components remain.

## Figures

Figure 1. Map of northern New Zealand; oil seep locations are indicated with various polygons (see legend in bottom-right corner for oil seep names); frontier basins most relevant to this study, as well as the established Taranaki Basin, are labeled; black lines indicate active plate boundary.

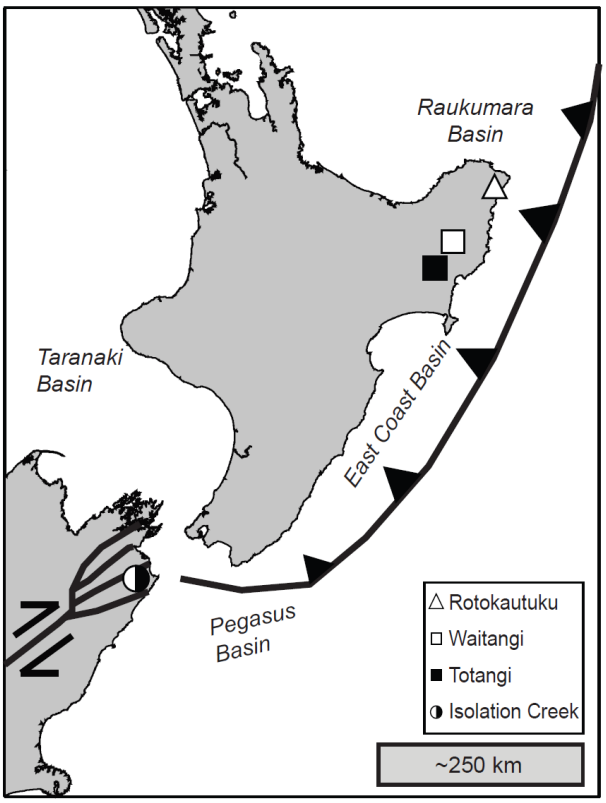

Figure 2. Wt. % sulfur versus $C_{35}$ homohopane index indicates more reducing depositional conditions for source rock of the southern oil samples and more oxic conditions for source rock(s) of the northern oil samples; symbols as in Figure 1.

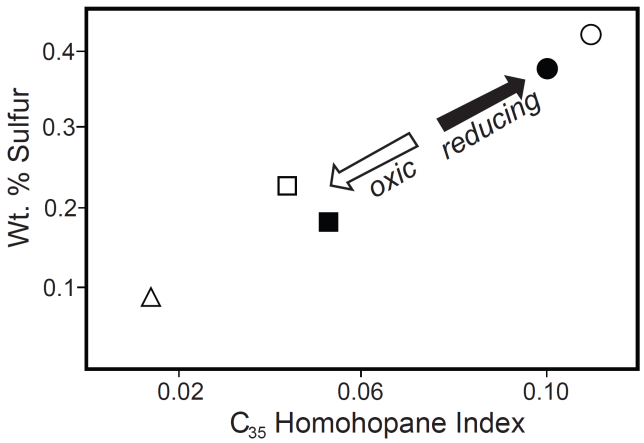


Figure 3. Various biomarker parameters all indicate a primarily shale source rock facies for these oil samples; symbols as in Figure 1.

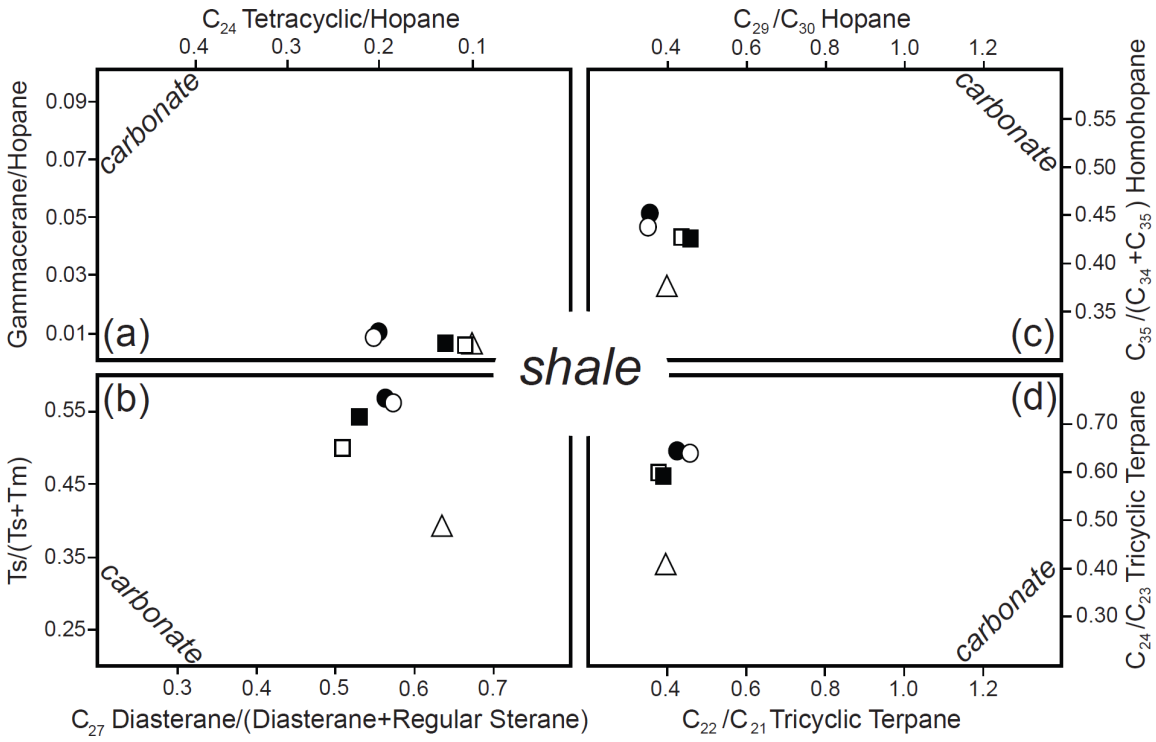

Figure 4. $\delta^{13}C_{saturates}$ versus $\delta^{13}C_{aromatics}$ of oils discussed herein plus numerous Cretaceous-Eocene oils from New Zealand, indicating the southern oil falls in line with Mid-Late and Late Cretaceous oils, whereas the northern oil samples fit with Eocene oils; Sofer (1984) line shown as dashed line.

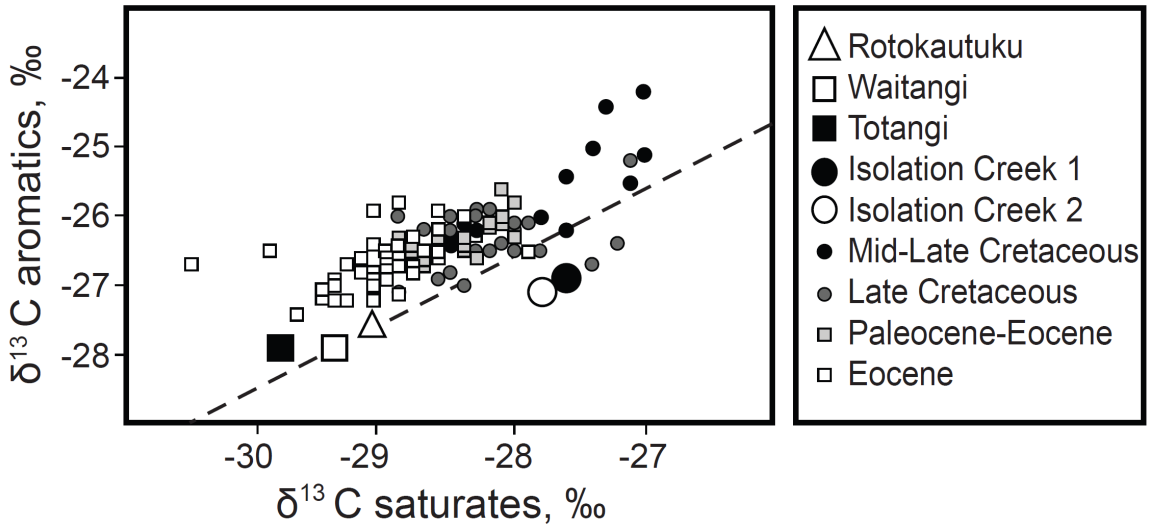


Figure 5. Abundance of $C_{26}$ 24-Nordiacholestanes relative to $C_{26}$ 27-Nordiacholestanes versus oleanane index; Cretaceous or younger age is indicated for all oil samples, however, a Cenozoic (and potentially Neogene) age is indicated for the northern oil samples according to $C_{26}$ Nordiacholestanes; oleanane abundances are also higher in the northern oil samples, suggesting a younger age relative to the southern oil samples; symbols as in Figure 1.

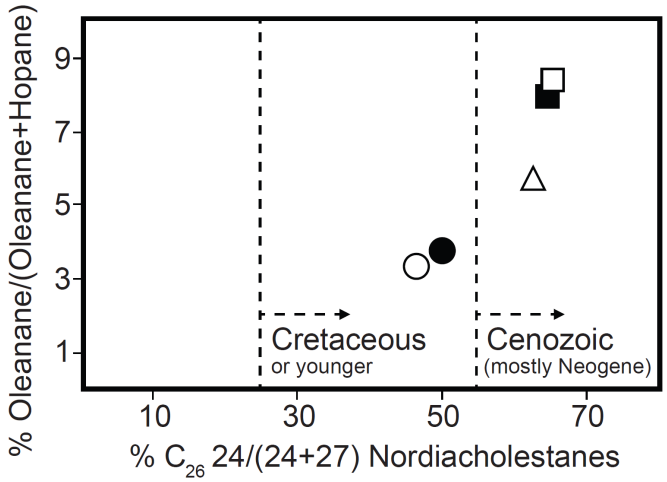

Figure 6. Representative m/z 217 fragmentograms of selected sterane distributions for the Waitangi and Isolation Creek (labelled "Kaikoura") samples illustrate the preservation of sterane biomarkers and the similarity of sterane/diasterane ratios for all samples (i.e., lack of biodegradation of steranes).

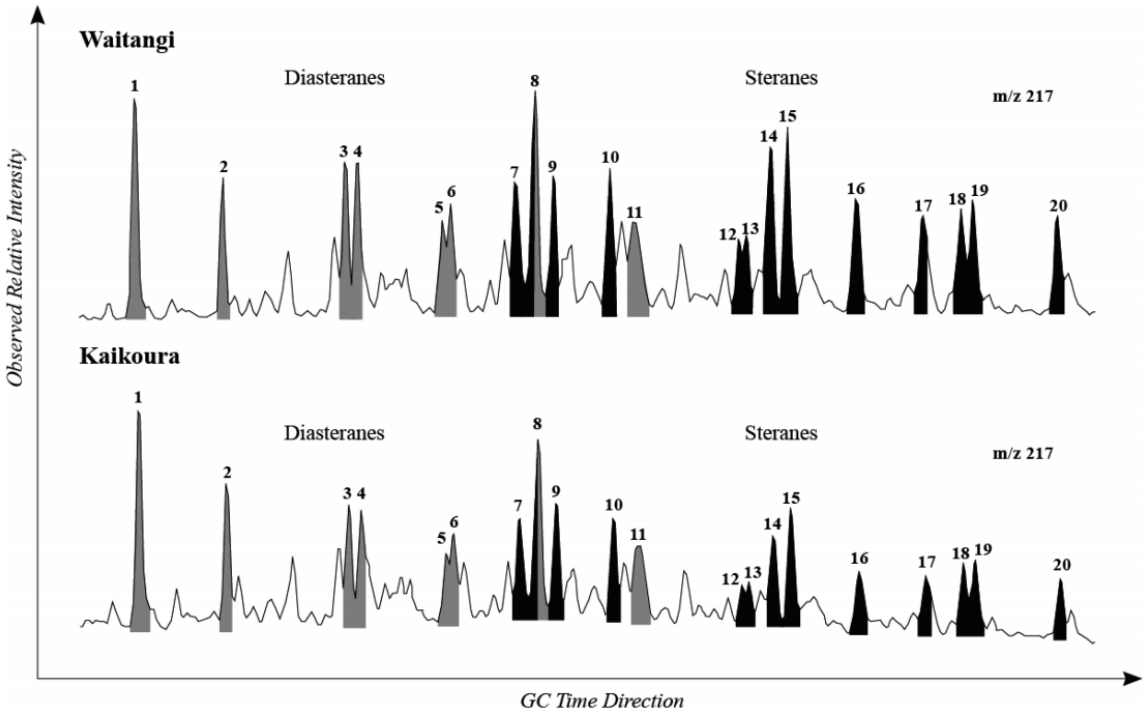

Figure 7. Concentrations of thermally stable diamondoids (methyldiamantanes) versus much less stable biomarkers (stigmastane) indicate thermal maturity and degree of cracking of oils, and reveal petroleum mixtures (note: “Kaikoura oil” is in fact a second Isolation Creek oil).

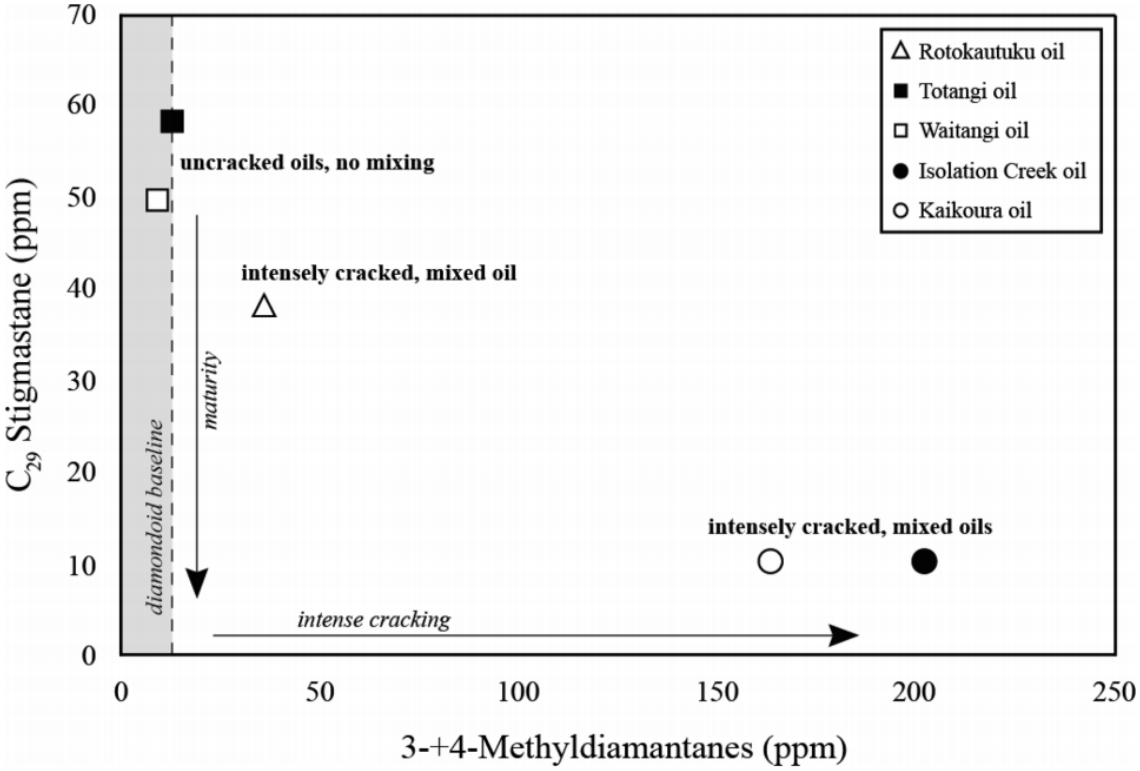

# CONSTRAINING UNCERTAINTY IN BASIN MODELING OF JEANNE D'ARC BASIN USING MEASURED DATA IN BAYESIAN NETWORKS

**Tanvi Chheda[1], Tapan Mukerji[2], Allegra Hosford Scheirer[1], and Stephan Graham[1]**
[1]*Department of Geological Sciences, Stanford University*
[2]*Department of Energy Resources Engineering, Stanford University*

## Introduction

In Basin and Petroleum System Modeling, because of the large number of input parameters, insufficient and imperfect data, among other things, there exists inherent uncertainty in modeling results. It is important to characterize this uncertainty and communicate predictions in a probabilistic manner. We propose a structured workflow to calibrate models to observed data and incorporate newly available data without the need to rerun basin models. We show this newer workflow for uncertainty reduction on 1D models created from well data in the Jeanne d'Arc basin in the prolific Grand Banks region offshore Newfoundland, Canada.

Organic rich Egret source rock was deposited in the Basin in Late Jurassic, followed by rifting due to opening of North Atlantic in Early Cretaceous, and episodic uplift and erosion that deposited many reservoir intervals until late Cretaceous. Albian-Aptian rifting from Greenland created major structural traps, and thick overburden was deposited in the Cenozoic (Grant and McAlpine, 1990; Richards *et al.*, 2010; Sinclair, 1993). Although this is the broad accepted geologic history, studies differ in the details. These different hypotheses are taken into account to create multiple basin models.

## Methodology

We use different possible heat flow scenarios (Baur *et al*., 2010) (Fig. 1), source rock parameters such as TOC, HI, and Kinetics, and amount of erosion scenarios to create 162 basin models at each individual well. Using the measured data from openly accessible Basins database from Natural Resources Canada, we calculated summary statistics for pressure, temperature, and vitrinite reflectance. We used these in the Bayesian Network (Fig. 2), along with predictions of these quantities from the models to select the subset of models that honored the data, thus obtaining the reduced uncertainty in model parameters.

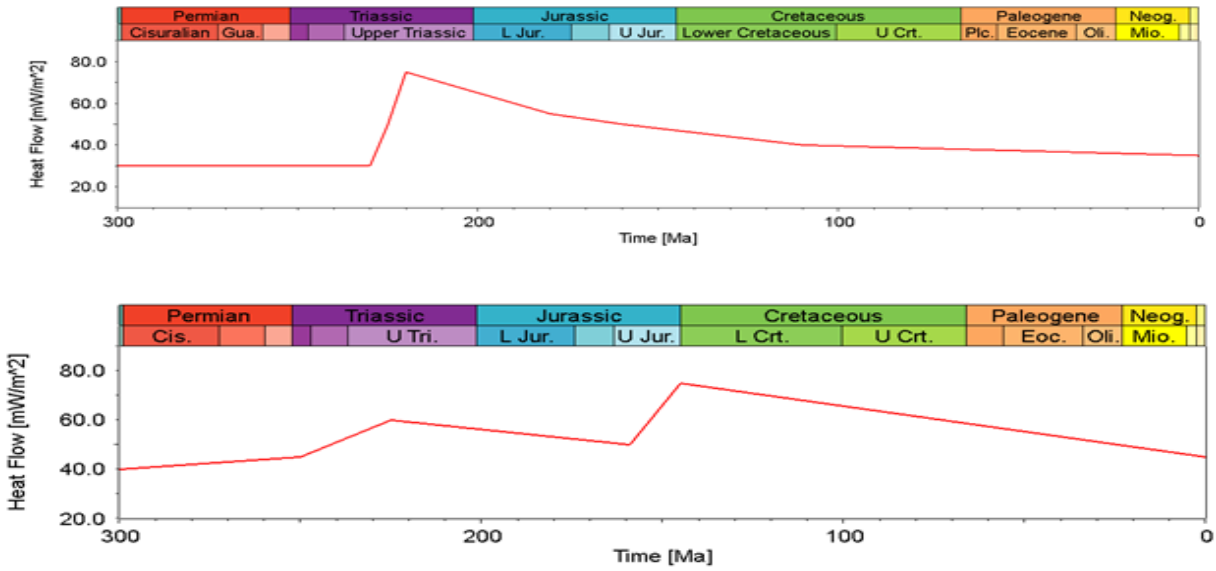


Figure 1: Basal heat flow scenarios due to uncertainty in contribution from different rifting phases.

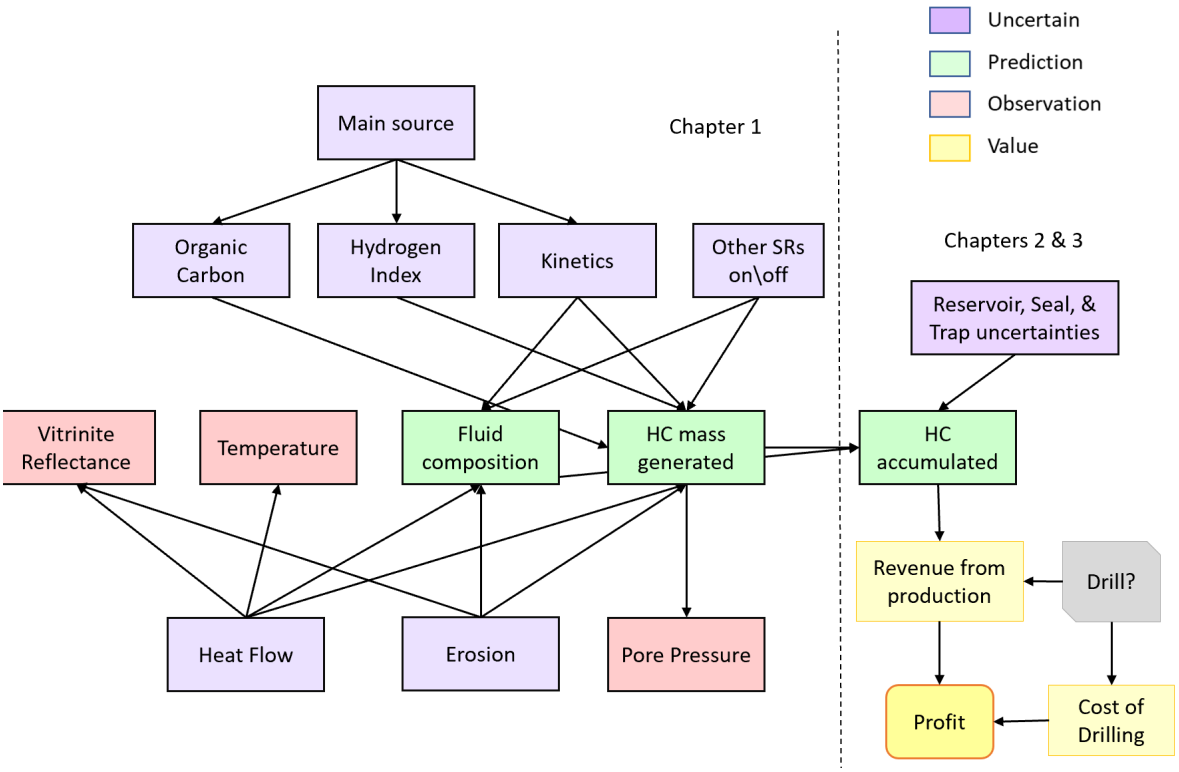


Figure 2: Simple Bayesian Network for the 1-D proof-of-concept experiment with sources of uncertainty (purple), calibration or evidence nodes (pink), and prediction variables (green)

**Basin model and results**

Figure 3b shows that the contribution of hydrocarbon mass from sources other than the Egret Formation is less than 10% of the mass generated by Egret Formation. The Transformation Ratio plot (Fig. 3a) shows that the Egret Formation source rock has

exhausted its generation potential, while Kimmeridgian and Fortune Bay Formation shale potential source rocks have generated less than 40% of their potential.

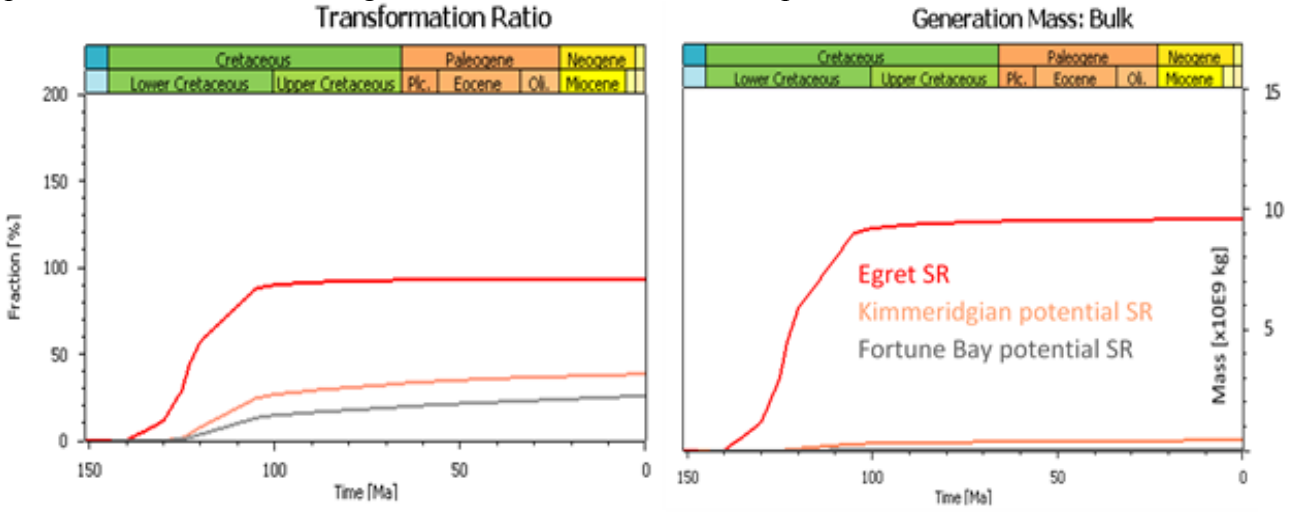


Figure 3: For Egret source rock (SR) and Kimmeridgian and Fortune Bay shale potential source rocks (A) Transformation Ratio and (B) Bulk petroleum mass generated.

Marginal distribution reflects the effect of one or more parameters solely by summing over all the other parameters. Amount of erosion has little effect on the charge (Fig. 4b) compared to total organic carbon (Fig. 4a). Figure 4c shows that for more than 9 megaton of hydrocarbon mass to be generated, the source rock would need to have a high TOC of >5%, while despite high TOC there is a chance that little hydrocarbon mass is generated, due to limiting hydrogen availability. Figure 4c assumed a uniform distribution for TOC, while figure 4d shows the impact of prior information, where higher probability was initially assigned to the amount of TOC measured in other parts of the basin, and a lower prior probability assigned to values deviating from it. The likelihood of median value for TOC increases for lower charge scenarios, but TOC >5% is still needed for very high charge.

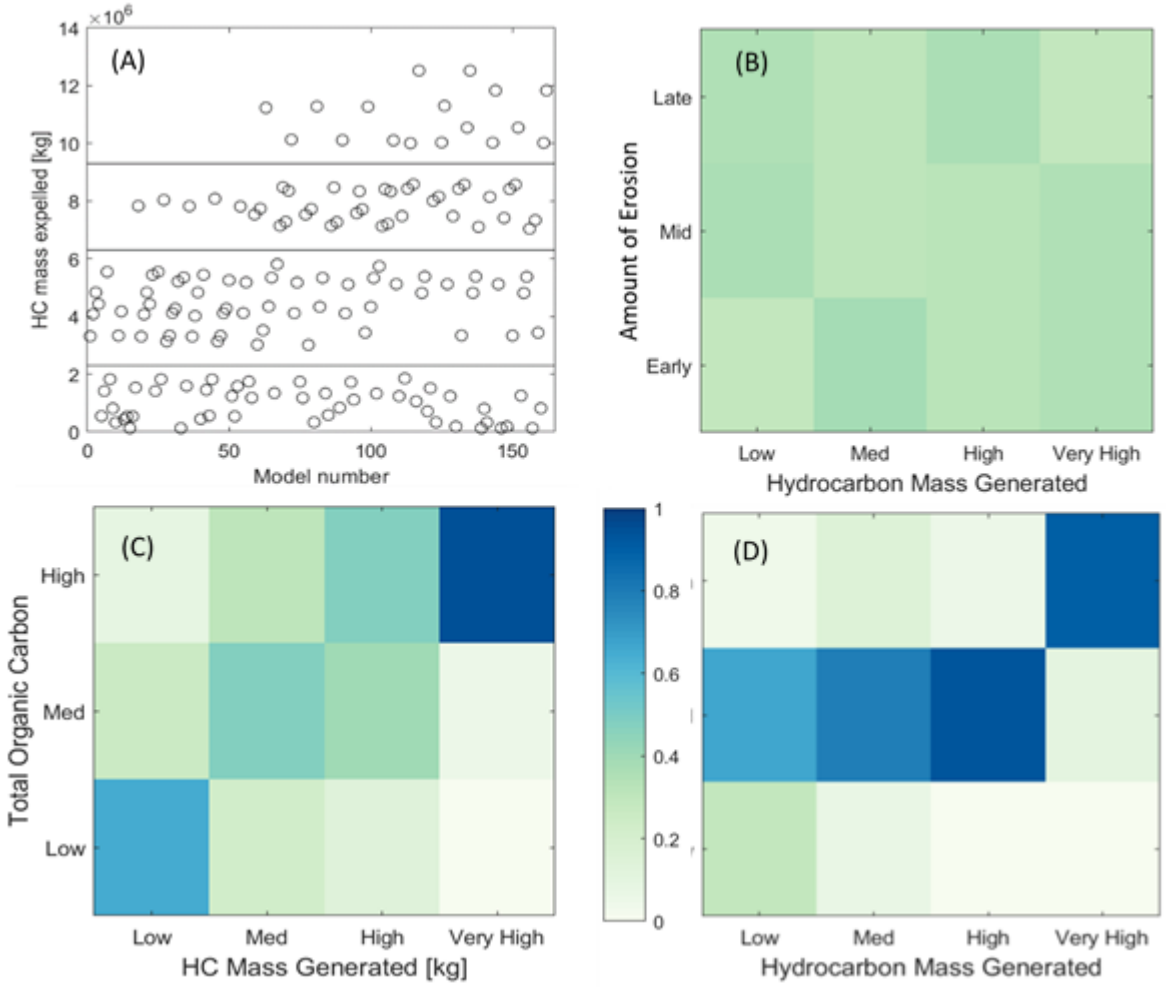


Figure 4: (A) K-means clustering algorithm to categorize mass of hydrocarbon generated (HCM) into categories Low, Medium, High, and Very High. (B) and (C) Sensitivity of prediction variable HCM to the model parameters. (D) Posterior probability of TOC given a prior [0.2, 0.6, 0.2] for Low, Medium, and High TOC.

**Summary and Conclusions**

In the future, this work will be extended to a 3D basin model with spatial uncertainties like lateral facies variation, migration pathways, and trapping mechanisms, and creating a newer structured decision-making process that is informed by a quantitative evaluation of risks and returns from exploration decisions. Although shown with the example of a conventional offshore basin in the east coast of Canada, this is fundamentally applicable to various basin types, locations, and decisions scenarios. The graphical formulation of Bayesian Network is an excellent communication tool that can incorporate expert knowledge and decision maker preferences. It also allows for modularity: risk components like source, reservoir, and trap can be evaluated separately as inputs from different teams as well as recombined for accumulation and level analyses at the management level in a large organization setting.

## References

Baur, F. *et al.* (2010) 'Basin modeling meets rift analysis - A numerical modeling study from the Jeanne d'Arc basin, offshore Newfoundland, Canada', *Marine and Petroleum Geology*, 27(3), pp. 585–599. doi: 10.1016/j.marpetgeo.2009.06.003.

Grant, A. C. and McAlpine, K. D. (1990) 'The Continental Margin around Newfoundland', in *Geology of the Continental Margin of Eastern Canada*, pp. 241–292. doi: 10.4095/132690.

Richards, F. W. *et al.* (2010) 'Reservoir connectivity analysis of a complex combination trap: Terra Nova Field, Jeanne d'Arc Basin, Newfoundland, Canada', *Geological Society, London, Special Publications*, 347(1), pp. 333–355. doi: 10.1144/SP347.19.

Sinclair, I. K. (1993) 'Tectonism: the dominant factor in mid-Cretaceous deposition in the Jeanne d'Arc Basin, Grand Banks', *Marine and Petroleum Geology*, 10(6), pp. 530–549. doi: 10.1016/0264-8172(93)90058-Z.

# OVERVIEW OF TOTAL-BPSM PROJECT ON PETROLEUM EXPULSION FROM VACA MUERTA SOURCE ROCK IN NEUQUÉN BASIN, ARGENTINA

**Mei Mei[1], Tapan Mukerji[1], Alan Burnham[1], Noelle Schoellkopf[2,3], Leslie Magoon[2], Allegra Hosford Scheirer[2], Johannes Wendebourg[4], Francois Gelin[4]**

[1]*Department of Energy Resources Engineering, Stanford University*

[2]*Department of Geological Sciences, Stanford University*

[3]*Schlumberger*

[4]*TOTAL E&P Research & Technology*

## Abstract

A new project was recently initiated between Total and BPSM at Stanford. The project will focus on basin modeling for the Vaca Muerta hybrid petroleum system in Neuquén Basin of Argentina (Fig. 1) to better understand the history of petroleum generation, expulsion, and migration. To achieve the goal, multidisciplinary methods including geology, geochemistry, rock physics, basin modeling, statistics, and petroleum engineering will be used. Heterogeneity in rock and geochemical properties and how these impacted petroleum expulsion and migration will be studied in detail. Numerical modeling and basin modeling based on dataset of core analysis, well log, and interpreted seismic will be integrated to better quantitatively analyze petroleum distribution with uncertainty analysis. Overall, the geological framework, dataset, and work plan will be reviewed in this talk.

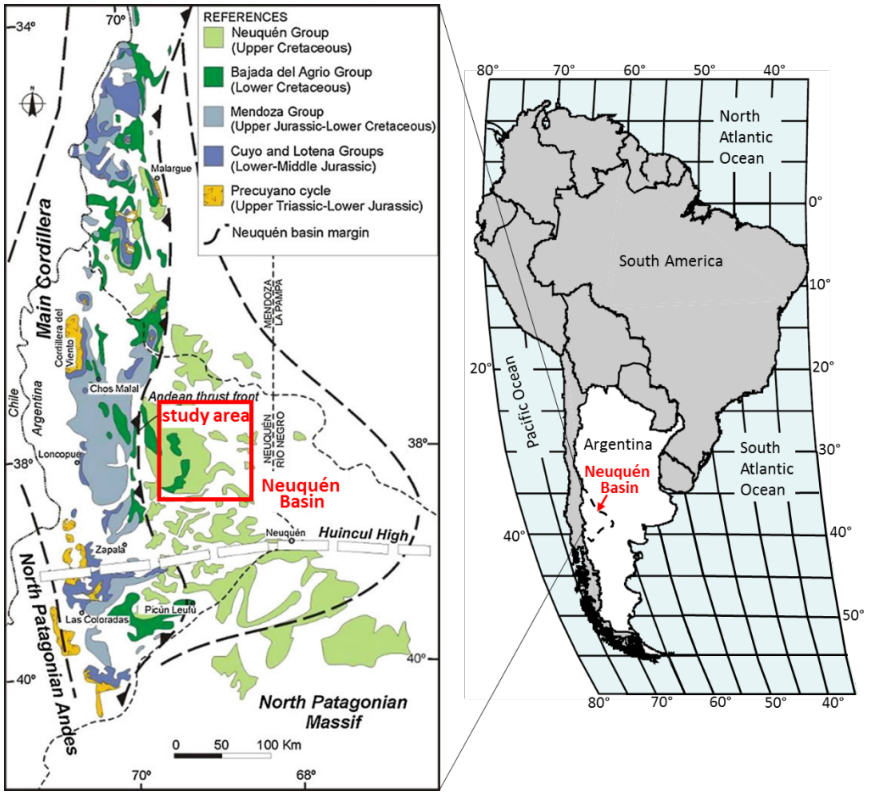


Fig. 1 Geological map of study area, central of Neuquén Basin, Argentina.

# GEOCHEMICAL PROPERTIES OF ORGANIC RICH MUDROCKS USING QUANTITATIVE SEISMIC INTERPRETATION

**Mustafa Al Ibrahim[1], Tapan Mukerji [1], Allegra Hosford Scheirer [2]**
[1]*Department of Energy Resources Engineering, Stanford University*
[2]*Department of Geological Sciences, Stanford University*

## Introduction

Estimating the lateral heterogeneity of geochemical properties of organic rich mudrocks is important for unconventional resource plays. Mature regions can rely on abundant well data to build empirical relationships and on traditional geostatistical methods to estimate properties between wells. However, well penetration in emerging plays are sparse and so these methods will not yield good results. In this case, quantitative seismic interpretation (QSI) might be helpful in estimating the desired properties. In this study, we use QSI based on rock physics template in estimating the uncertainty of the geochemical properties of organic mudrocks of the Shublik Formation, North Slope, Alaska. A rock physics template incorporating lithology, pore fraction, kerogen fraction, and maturation (Figure 1) is constructed and validated using well data. The template clearly shows that the inversion problem is non-unique. Inverted impedances cubes are estimated from three seismic angle gathers (near with angles between 0° and 15°, mid with angle gather between 15° and 30°, and far with angle gathers between 30° and 45°). The inversion is done using a model based implementation with an initial earth model derived from the seismic velocity model used in the processing phase (Figure 2). By combining the rock physics template and the results of seismic inversion, multiple realizations of total organic content (TOC) are generated (e.g., Figure 3). Standard deviation maps are calculated to illustrate the confidence in the estimation. These results will be used as an input for basin and petroleum system modeling.

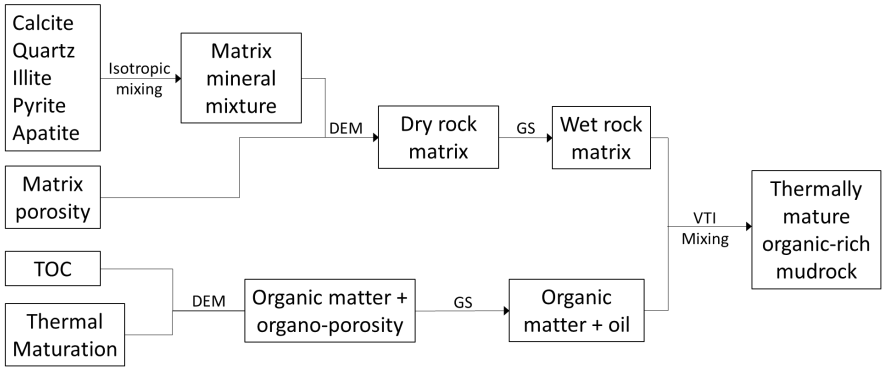


Figure 1: The procedure followed to build the rock physics template of thermally mature organic rich mudrocks.

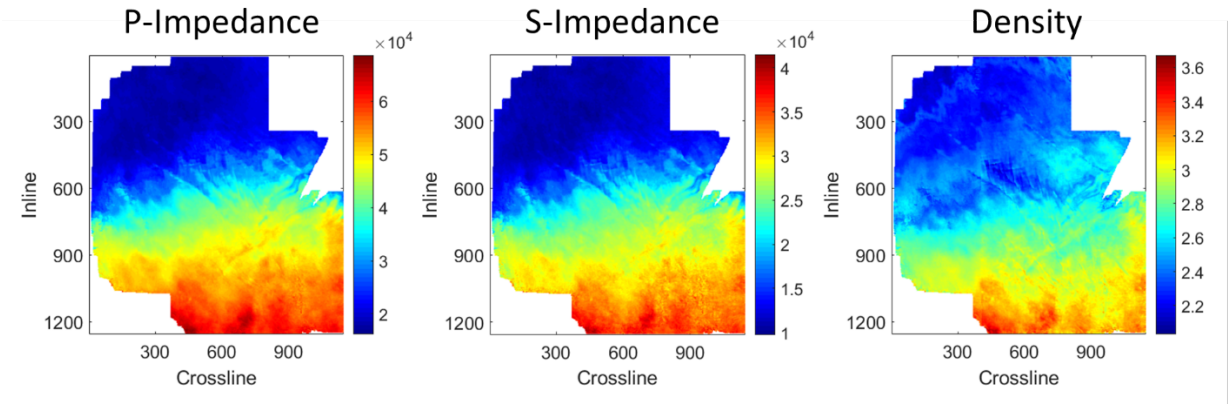


Figure 2: Pre-stack inversion results on top of the Shublik Formation.

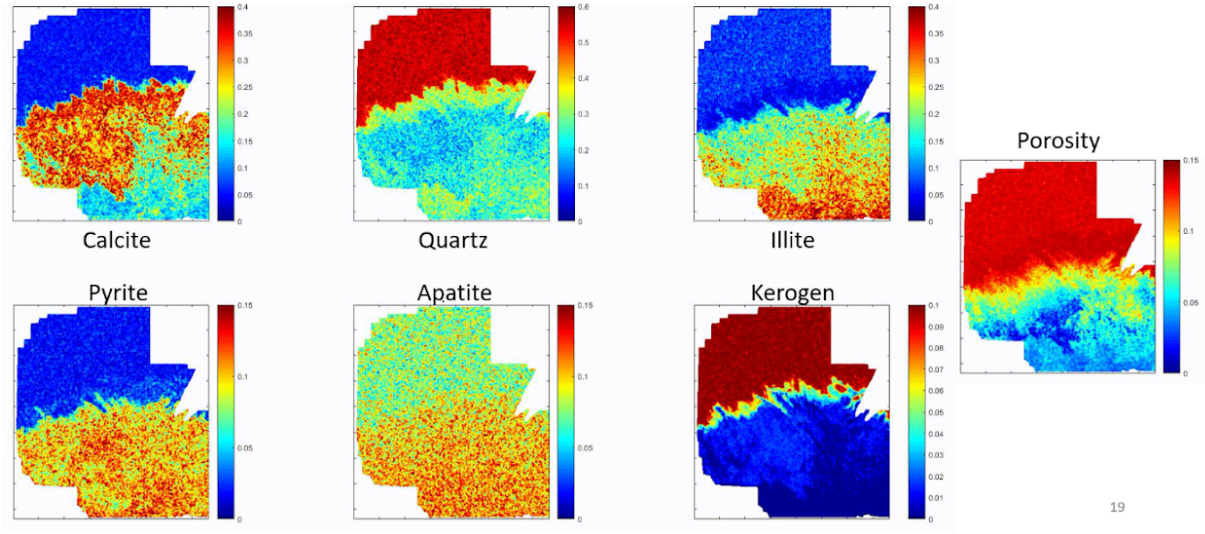


Figure 3: One realization of the estimate of the different geochemical properties.

## Integrating basin modeling and seismic imaging for uncertainty reduction

**Anshuman Pradhan[1], Huy Q. Le[2], Nader C. Dutta[2] and Tapan Mukerji[1]**
[1]*Department of Energy Resources Engineering, Stanford University*
[2]*Department of Geophysics, Stanford University*

A critical input to any basin-modeling endeavor are the present-day geometries of key geologic horizons. This is generally achieved by identifying horizons in seismic data, be it on a 2D section or 3D volume. However, the depths and spatial locations of the horizons as observed in the seismic image are highly dependent on the velocity model used for seismic depth migration or the imaging algorithm used. Varying structural geometries of geologic features will lead to varying structural history of the basin and consequently different thermal or pressure history. Thus, the nuances of the seismic imaging workflow will critically control the outcome of the basin modeling. On the other hand, seismic imaging itself is strongly controlled by the geo-history of the basin because compaction and over-pressuring will affect the velocity of the subsurface. Thus, it is desirable to ensure that the basin modeling and seismic imaging workflows integrate these mutual constraints. However, integrating constraints from disparate disciplines such as those listed above comes with several challenges. Discipline-specific uncertainties exist in each workflow and thus it is imperative to ensure that these uncertainties are consistently propagated. In this work, we present a Bayesian framework which facilitates integrated yet rigorous quantification of uncertainties associated with basin modeling and seismic imaging.

Equation 1 shown below captures the essence of our proposed methodology. In a Bayesian setting, our goal is to generate samples of the uncertain basin modeling parameters and velocity model from the posterior distribution, shown on the L.H.S. of Equation 1, given the well data $d_1$ and seismic data $d_2$. We use Bayes rule to express the posterior in terms of the prior distributions and likelihood functions. We state our prior uncertainties on relevant basin modeling parameters denoted by the random vector $B$. $B$ could include various parameters such as mechanical compaction curves or permeability models or boundary conditions. The physical model linking the velocity model of the earth $V$ and $B$ is specified as the combination of the basin model and an appropriate rock physics model. $f(d_1)$ is the basin modeling likelihood term, which can be estimated using the fit of the basin modeling outputs to the well calibration data. $f(d_2)$ is the seismic likelihood term which will be estimated from the flatness of the common image gathers generated post seismic migration.

$$\text{Equation-1:} \quad f(B, V \mid d_1, d_2) \propto f(B) f(V) f(B) f(B)$$

Here, $f(.)$ denotes the probability density function.

We propose to use the rejection sampling method to generate the desired posterior samples. We will implement our workflow by building a 2D basin model using the EDragon dataset in offshore Louisiana and performing reverse time migration of the pre-stack seismic data.

**BASIN-SCALE INELASTIC DEFORMATION OF SEAL AND SOURCE ROCK AND ITS IMPACT ON OVERPRESSURE PREDICTION**

**Laainam Chaipornkaew[1], Tapan Mukerji[2], Steve Graham[1]**
[1]*Department of Geological Sciences, Stanford University*
[2] *Department of Energy Resources Engineering, Stanford University*

Basin and Petroleum System Modeling (BPSM) describes the evolution of stress in sedimentary basins through geologic time (Al-Hajeri et al., 2009; Hantschel and Kauerauf, 2009); This approach shows great potential in pore pressure prediction, especially when compared to other techniques that only consider in-situ stress conditions such as seismic-derived. However, several published studies using BPSM techniques in structurally complex regions show inaccurate pressure predictions due to a lack of advanced rock failure modeling (Neumaier et al., 2014; Burgreen-Chan et al., 2016). At basin-scale, sedimentary rocks experience inelastic deformation accompanied by shear-enhanced compaction under increasing confining pressure (Byerlee, 1968, Wong and Baud, 2012; Nicksiar and Martin, 2013). Recent studies (Gutierrez et al., 2001; Rutqvist et al., 2002; Minkoff et al., 2003) attempt to incorporate more realistic deformation at the field-scale, in which fluid flow, deformation, and temperature fields are (loosely- to partially-) coupled. This research tracks evolving stress conditions in sedimentary rocks at the basin-scale using a fully-coupled fluid flow and deformation simulator (Obradors-Prats et al., 2017; Crook et al., 2018).

Inelastic deformation affects seal and source rock rather differently, especially in relation to overpressure mechanisms. Deformed seals disrupt hydrocarbon retention, leading to pressure dissipation. Instead, deformed source rocks enhance hydrocarbon expulsion, possibly leading to pressure generation. Our previous work modeling inelastically deformed seal rocks achieves more realistic overpressure prediction in the synthetic dataset with geologic settings similar to that of East Coast basin of New Zealand. This work switches gears to explore inelastically deformed source rocks, aiming to explore additional mechanisms that contributes to overpressure generation for a relatively old basin like the Anadarko.

A couple of research questions include- How generated hydrocarbon escapes from source rocks? Is expulsion efficiency dominated more by geochemical kinetics or by transport properties such as diffusion by Darcy flow and bulk flow via permeable pathways? My work will focus on the latter though it is likely that multiple mechanisms operate at different time and stage of maturation (Kobchenko, 2013). Experiments in low permeability shales highlight the effects of deformation during kerogen decomposition, fluid expulsion, and fracture evolution (Burrus et al., 1993; Slatt and O'Brien, 2011; Ma et al., 2017). See Figure 1, 2. We will apply the established workflow for deformed low-permeability seal to low-permeability source rock. The ultimate goal is to track how it would affect expulsion modeling especially in relation to added overpressure generation.

The Anadarko Basin is extensively overpressured and compartmentalized within a completely sealed Mega-Compartment Complex (Al-Shaieb et al. 1994a). Though possible drivers to this phenomenon could be hydrocarbon generation, capillary sealing, or disequilibrium compaction, to date, there is still no strong agreement on mechanisms that could add up to existing anomalous overpressure in such an old and exposed basin (Lee and Deming, 2002; Cranganu and Villa, 2006). Because the Woodford shale marks a distinct transition between abnormal-high overpressure trend in the overlying rocks and perfectly hydrostatic trend in the underlying Hunton Group (Figure 3), it is a natural choice for us to explore the prolific Woodford shale again.

Upper and middle Woodford are reported to have high fracture densities possibly due to organic-rich and high-quartz intervals (Romina and Slatt, 2016; Ghosh et al., 2017). Major uplifts surrounding the Anadarko basin could impact subsequent fracturing and consequently these fractured source rocks may assist more optimistic expulsion volume, and additional overpressure generation, than traditional models. Unlike deformed seals that allow hydrocarbon to leave the system, deformed source rocks allow more hydrocarbon to enter the system. Hence, ability to realistically model inelastic deformation in shale as seal rocks and source rocks are critical to basin and petroleum system modeling.

**References**


Al-Hajeri, M. M., M. Al Saeed, J. Derks, T. Fuchs, T. Hantschel, A. Kauerauf, M. Neumaier, O. Schenk, O. Swientek, and N. Tessen, 2009, Basin and petroleum system modeling: Oilfield Review, v. 21, no. 2, p. 14–29.

Al-Shaieb, Z., J. O. Puckette, A. A. Abdalla, and P. B. Ely, 1994a, Megacompartment complex in the Anadarko basin: a completely sealed overpressured phenomenon: Basin Compartments and Seals, p. 55–68.

Al-Shaieb, Z., J. O. Puckette, A. A. Abdalla, and P. B. Ely, 1994b, Three levels of compartmentation within the overpressured interval of the Anadarko Basin: Basin Compartments and Seals, p. 69–83, doi:10.1306/F4C8DAE0-1712-11D7-8645000102C1865D.

Burgreen-Chan, B., K. E. Meisling, and S. Graham, 2016, Basin and petroleum system modelling of the East Coast Basin, New Zealand: a test of overpressure scenarios in a convergent margin: Basin Research, v. 28, no. 4, p. 536–567, doi:10.1111/bre.12121.

Burrus, J., K. G. Osadetz, J.-M. Gaulier, E. Brosse, B. Doligez, G. C. de Janvry, J. Barlier, and K. Visser, 1993, Source rock permeability and petroleum expulsion efficiency: modelling examples from the Mahakam Delta, the Williston Basin and the Paris Basin, *in* Petroleum Geology of Northwest Europe: Proceedings of the 4th Conference on Petroleum Geology of NW. Europe, at the Barbican Centre, London: doi:10.1144/0041317.

Byerlee, J. D., 1968, Brittle-ductile transition in rocks: Journal of Geophysical Research, v. 73, no. 14, p. 4741–4750.

Cranganu, C., and M. a Villa, 2006, Capillary Sealing as an Overpressure Mechanism in the Anadarko Basin: Search and Discovery.

Crook, A. J. L., J. Obradors-Prats, D. Somer, D. Peric, P. Lovely, and M. Kacewicz, 2018, Towards an integrated restoration/forward geomechanical modelling workflow for basin evolution prediction: Oil & Gas Science and Technology - Rev. IFP Energies nouvelles, v. 73.

Ghosh, S., J. N. Hooker, C. P. Bontempi, and R. M. Slatt, 2017, High-resolution stratigraphic characterization of natural fracture attributes in the Woodford Shale, Arbuckle Wilderness and US-77D Outcrops, Murray County, Oklahoma: Interpretation, doi:10.1190/int-2017-0056.1.

Gilbert, M. C., 1992, Speculations on the Origin of the Anadarko Basin, *in* R. Mason, ed., Basement Tectonics 7: Proceedings of the Seventh International Conference on Basement Tectonics, held in Kingston, Ontario, Canada, August 1987: Dordrecht, Springer Netherlands, p. 195–208, doi:10.1007/978-94-017-0833-3_14.

Gutierrez, M., R. W. Lewis, and I. Masters, 2001, Petroleum Reservoir Simulation Coupling Fluid Flow and Geomechanics: SPE Reservoir Evaluation & Engineering, v. 4, no. 3, p. 164–172, doi:10.2118/72095-PA.

Hantschel, T., and A. I. Kauerauf, 2009, Fundamentals of basin and petroleum systems modeling: 1-476 p., doi:10.1007/978-3-540-72318-9.

Hantschel, T., B. Wygrala, M. Fuecker, and A. Neber, 2011, Modeling Basin-scale Geomechanics Through Geological Time: International Petroleum Technology Conference, no. i, p. 6, doi:10.2523/15286-MS.

Kobchenko, M., 2013, Fracturing of tight rocks during internal fluid production: implications for primary migration: University of Oslo.

Kobchenko, M., H. Panahi, F. Renard, D. K. Dysthe, A. Malthe-Srenssen, A. Mazzini, J. Scheibert, B. Jamtveit, and P. Meakin, 2011, 4D imaging of fracturing in organic-rich shales during heating: Journal of Geophysical Research: Solid Earth, doi:10.1029/2011JB008565.

Lee, Y., and D. Deming, 2002, Overpressures in the Anadarko basin, southwestern Oklahoma: Static or dynamic: AAPG Bulletin, v. 86, no. 1, p. 145–160, doi:10.1306/61EEDA62-173E-11D7-8645000102C1865D.

Ma, C. et al., 2017, Controls of hydrocarbon generation on the development of expulsion fractures in organic-rich shale: Based on the Paleogene Shahejie Formation in the Jiyang Depression, Bohai Bay Basin, East China: Marine and Petroleum Geology, v. 86, p. 1406–1416, doi:10.1016/J.MARPETGEO.2017.07.035.

Meng, Z., J. Zhang, and S. Peng, 2006, Influence of sedimentary environments on mechanical properties of clastic rocks: Environmental Geology, v. 51, no. 1, p. 113–120, doi:10.1007/s00254-006-0309-y.

Minkoff, S. E., C. M. Stone, S. Bryant, M. Peszynska, and M. F. Wheeler, 2003, Coupled fluid flow and geomechanical deformation modeling: Journal of Petroleum Science and Engineering, v. 38, no. 1–2, p. 37–56, doi:10.1016/S0920-4105(03)00021-4.

Neumaier, M., R. Littke, T. Hantschel, L. Maerten, J. P. Joonnekindt, and P. Kukla,

2014, Integrated charge and seal assessment in the Monagas fold and thrust belt of Venezuela: AAPG Bulletin, doi:10.1306/01131412157.

Obradors-Prats, J., M. Rouainia, A. C. Aplin, and A. J. L. Crook, 2017, Assessing the implications of tectonic compaction on pore pressure using a coupled geomechanical approach: Marine and Petroleum Geology, doi:10.1016/j.marpetgeo.2016.10.017.

Romina, P., and R. Slatt, 2016, Understanding of natural fractures in the Woodford shale to improve hydrocarbon production, *in* SEG International Conference and Exhibition: p. 356.

Rutqvist, J., Y.-S. Wu, C.-F. Tsang, and G. Bodvarsson, 2002, A modeling approach for analysis of coupled multiphase fluid flow, heat transfer, and deformation in fractured porous rock: International Journal of Rock Mechanics and Mining Sciences, v. 39, no. 4, p. 429–442, doi:10.1016/S1365-1609(02)00022-9.

Slatt, R. M., and N. R. O'Brien, 2011, Pore types in the Barnett and Woodford gas shales: Contribution to understanding gas storage and migration pathways in fine-grained rocks: AAPG Bulletin, doi:10.1306/03301110145.

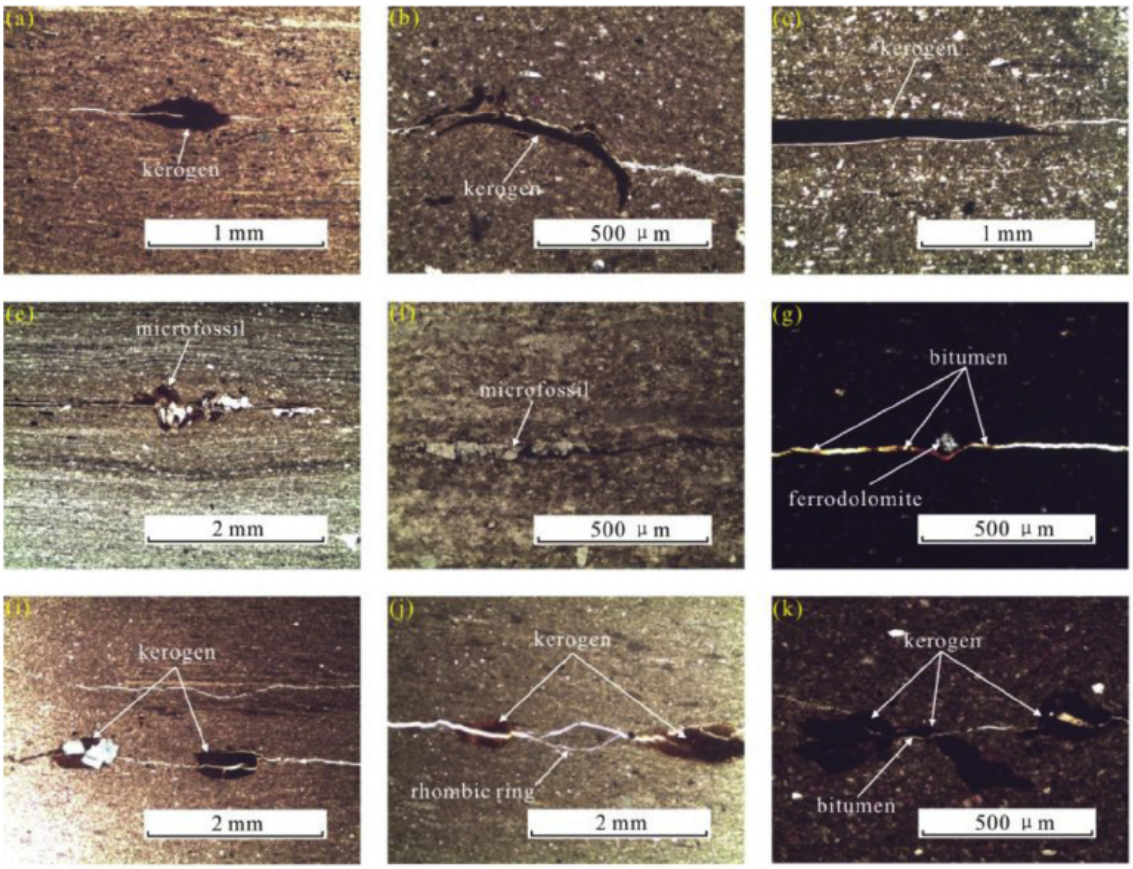


**Figure 1:** Characteristics of the expulsion fracture in shale. Fractures are observed to have close association with kerogens in various forms (modified from Ma et al., 2017).

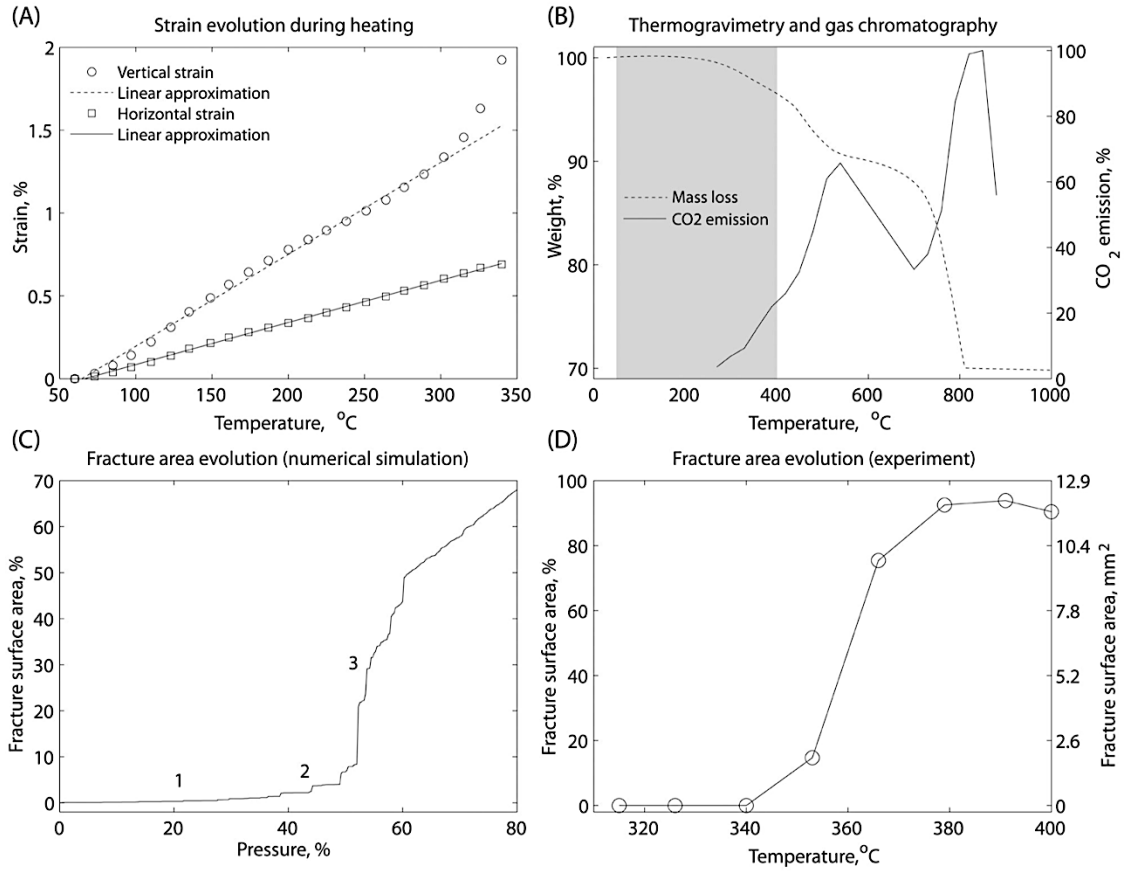


**Figure 2:** Observation from organic-rich shales during heating experiment (Kobchenko et al., 2011), which highlights the effects of deformation during kerogen decomposition, CO2 production, fluid expulsion, and fracture evolution.

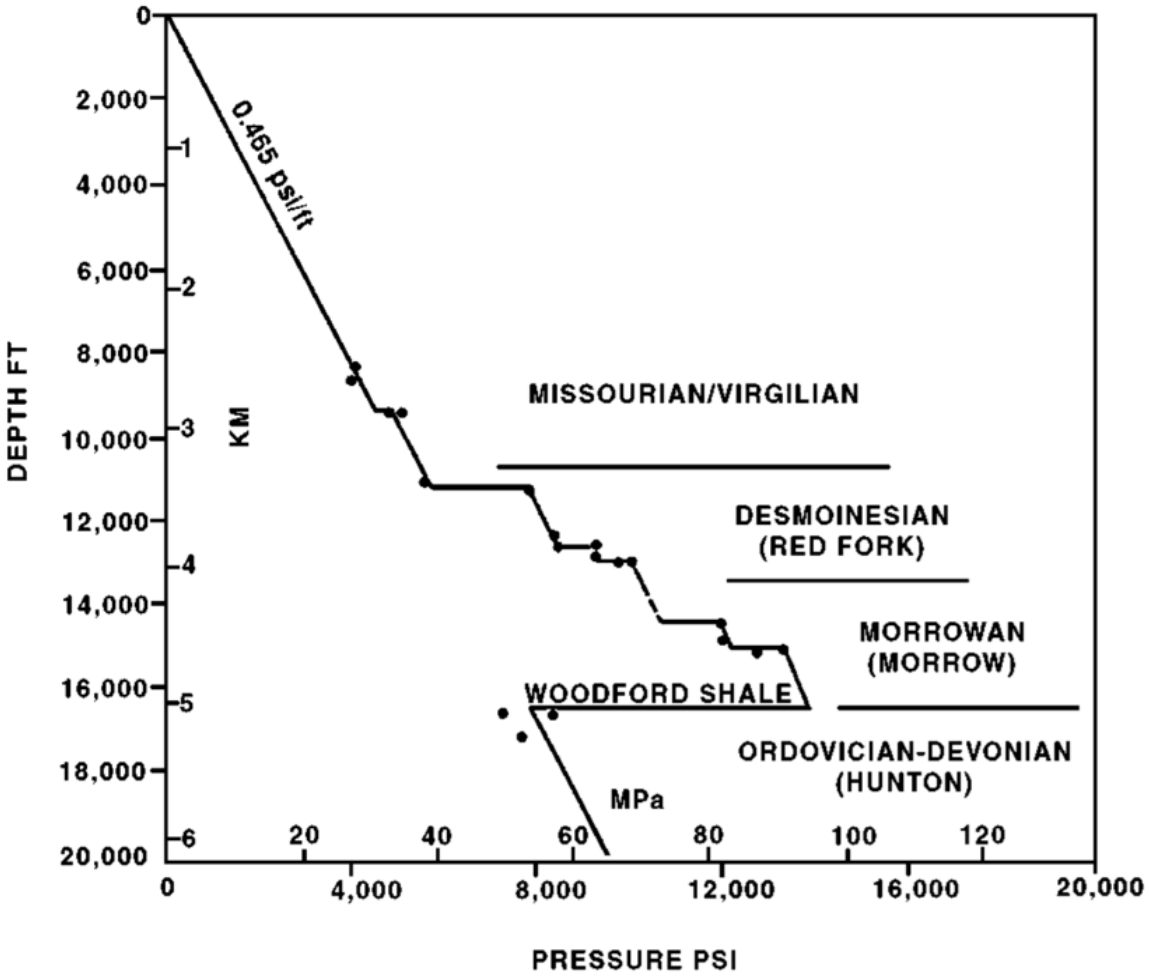


**Figure 3**: Pressure-depth profile identifying abnormally high overpressured reservoirs above the Woodford shale and normal pressure gradients in the underlying Hunton Group (Al-Shaieb et al., 1994a).

# FAULT SEALING IN OIL AND GAS EXPLORATION: EXISTING METHODS AND RESEARCH MOTIVATION

**Anatoly Aseev[1], Allegra Hosford Scheirer[1] and Ebbe H. Hartz[2]**
[1]*Department of Geological Sciences, Stanford University*
[2]*Aker BP, Norway*

## Introduction

Most obvious exploration targets—large-scale anticlines—have already been drilled and prospected. Thus, modern exploration targets tend to be more structurally complex with faults of different scales and properties. Sealing properties of the faults control fault plane permeability and the corresponding column height of faulted hydrocarbon accumulation. Currently, hydrocarbon explorationists use several approaches (Sperrevik et al., 2002; Bretan et al., 2003; Yielding et al., 2010) for estimation of hydrocarbon column-heights, which are based on clay smear of the fault plane (Vrolijk et al., 2016), shale gauge ratio (Yielding et al., 1997) and depth of the fault (Figure 1). These approaches produce questionable results (Figure 2) because they are based on empirically derived equations from limited types of faults and are missing critical factors affecting faults permeability. This results in high uncertainties in estimation of hydrocarbon column-heights.

This work encompasses an overview of the factors affecting fault permeabilities, and a proposal to study uncertainty and sensitivity of those factors. Understanding these factors are critical for calculating hydrocarbon column heights. Based on the results of uncertainty and sensitivity study of fault sealing factors, a workflow for estimation of hydrocarbon column-heights in faulted traps will be formulated. The workflow will be tested on faulted petroleum systems of the South Viking Graben, North Sea.

## Proposed research

The proposed research comprises three parts: i) exploratory analysis of factors affecting fault permeability, ii) uncertainty and sensitivity analysis of fault sealing factors, and iii) reducing fault sealing uncertainties in central North Sea using petroleum systems simulations. The corresponding overview of each part is addressed below.

i) The current fault sealing techniques ignore many significant factors affecting fault permeability, such as dynamic factors (Wiprut and Zoback, 2002), hydrodynamic flow (Manzocchi and Childs, 2013), fault type, fault rock alteration, structural uncertainties etc. Thus, the first part of the work aims to conduct exploratory analysis of these factors by using literature data, data mining on faulted accumulations database from Norwegian Continental Shelf and California (Division of Oil, Gas, 1998), and exploring statistical learning techniques for improvement the existing formulations (Sperrevik et al., 2002; Yielding et al., 2010).

ii) In order to capture the effect of varying fault sealing parameters, this work proposes to perform statistically sufficient set of 2D basin modeling simulations of the migration processes through fault using synthetic dataset. The sensitivity of fault sealing parameters will be evaluated based on the results of simulations. These simulations will be performed using PetroMod software and will combine all the factors affecting faults permeability with two distinct fluid migration methods – Darcy's flow and Invasion Percolation (critical capillary pressure) in Figure 3 (Hantschel and Kauerauf, 2009). The sensitivity analysis of the simulations will facilitate in highlighting the most critical factors affecting fault permeability or fluid column heights.

iii) A workflow will be formulated for estimation of hydrocarbon column-heights in the faulted traps. The workflow will be tested on one of the faulted oil discoveries in Viking Graben area, North Sea (Figure 4), where more than 75% of the exploration wells failure is due to problems with charge and seal.

**Acknowledgements**

I would like to thank Aker BP Company for providing geological data for the upcoming research, and Dr. Ebbe H. Hartz personally for inspiration and support.

**References**

Ahmadi, Z., M. Sawyers, S. E. M. G. Kenyon-Roberts, D. Paleocene. In: Evans, K. K.A, J. Fugelli, and P. (eds) 235-259 G. C. A. A. Bathurst, 2003, The Millenium Atlas: Petroleum geology of the central and northern North sea: doi:DOI: 10.1017/S0016756803218124.

Bretan, P., G. Yielding, and H. Jones, 2003, Using calibrated shale gouge ratio to estimate hydrocarbon column heights: American Association of Petroleum Geologists Bulletin, doi:10.1306/08010201128.

Division of Oil, Gas, and G. R., 1998, CALIFORNIA OIL & GAS FIELDS Volume 1 - Central California: CALIFORNIA OIL & GAS FIELDS Volume 1 - Central California.

Hantschel, T., and A. I. Kauerauf, 2009, Fundamentals of basin and petroleum systems modeling: doi:10.1007/978-3-540-72318-9.

Manzocchi, T., and C. Childs, 2013, Quantification of hydrodynamic effects on capillary seal capacity: Petroleum Geoscience, doi:10.1144/petgeo2012-005.

Sperrevik, S., P. A. Gillespie, Q. J. Fisher, T. Halvorsen, and R. J. Knipe, 2002, Empirical estimation of fault rock properties: Norwegian Petroleum Society Special Publications, doi:10.1016/S0928-8937(02)80010-8.

Vrolijk, P. J., J. L. Urai, and M. Kettermann, 2016, Clay smear: Review of mechanisms

and applications: doi:10.1016/j.jsg.2015.09.006.

Wiprut, D., and M. D. Zoback, 2002, Fault reactivation, leakage potential, and hydrocarbon column heights in the northern north sea: Norwegian Petroleum Society Special Publications, doi:10.1016/S0928-8937(02)80016-9.

Yielding, G., P. Bretan, and B. Freeman, 2010, Fault seal calibration: a brief review: Geological Society, London, Special Publications, doi:10.1144/SP347.14.

Yielding, G., B. Freeman, and D. T. Needham, 1997, Quantitative fault seal prediction: AAPG Bulletin, doi:10.1306/522B498D-1727-11D7-8645000102C1865D.

**Figures**

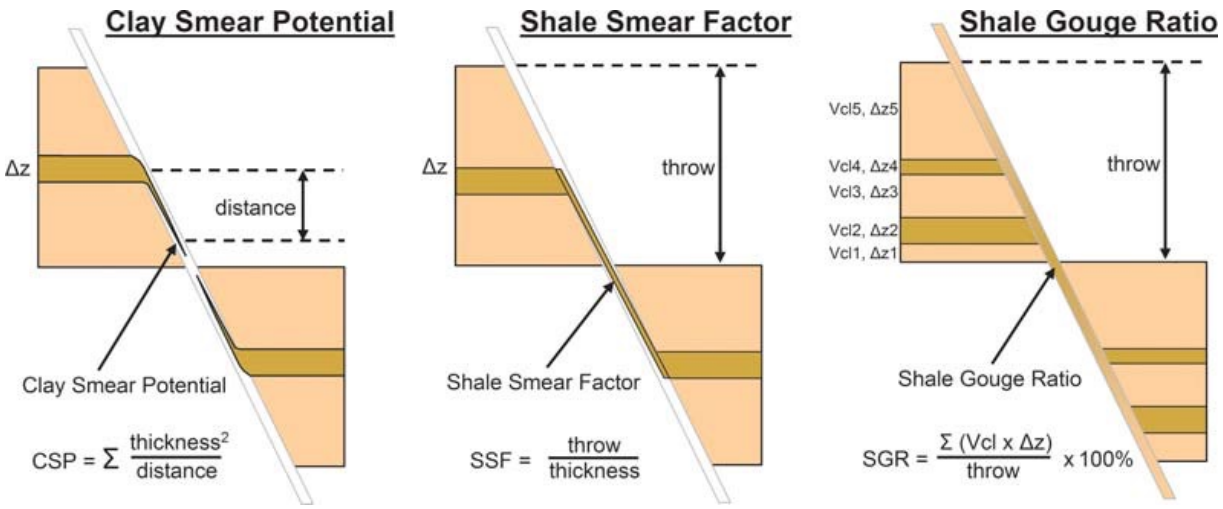


**Figure 1**. The three main fault-seal algorithms (after Yielding et al., 2010)

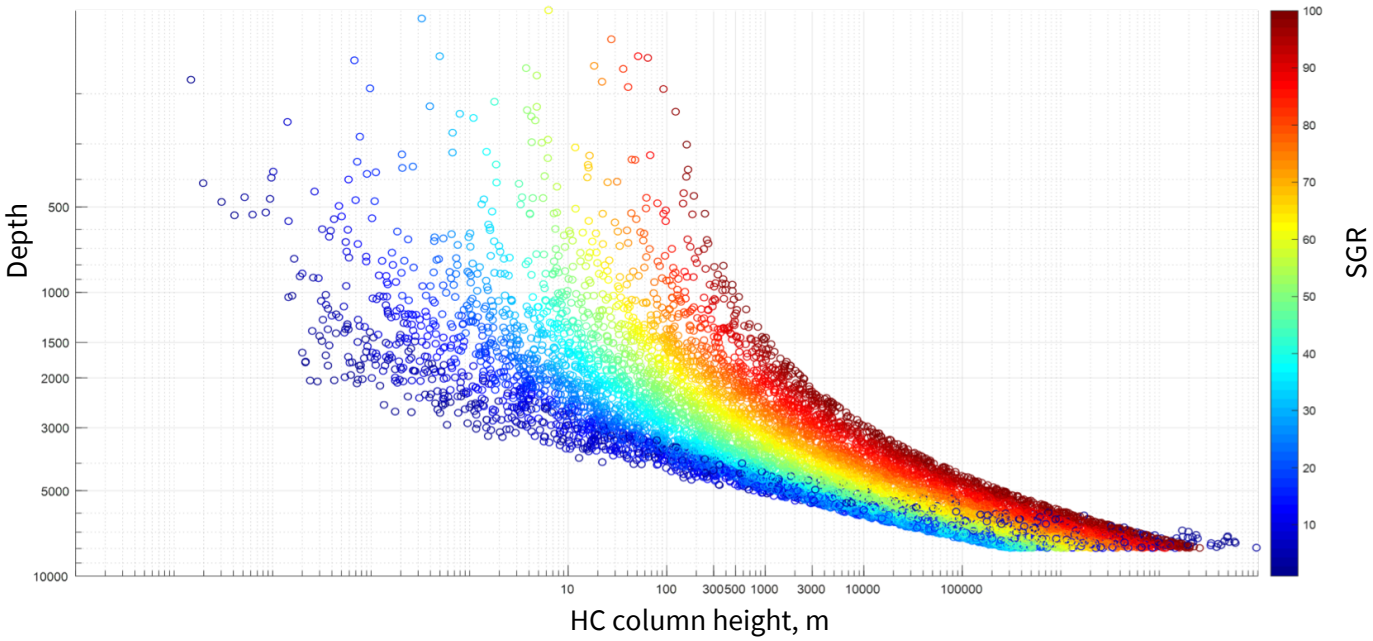


**Figure 2**. Eight-thousand simulations of hydrocarbon column-heights using algorithm by Sperrevik et al. (2002).

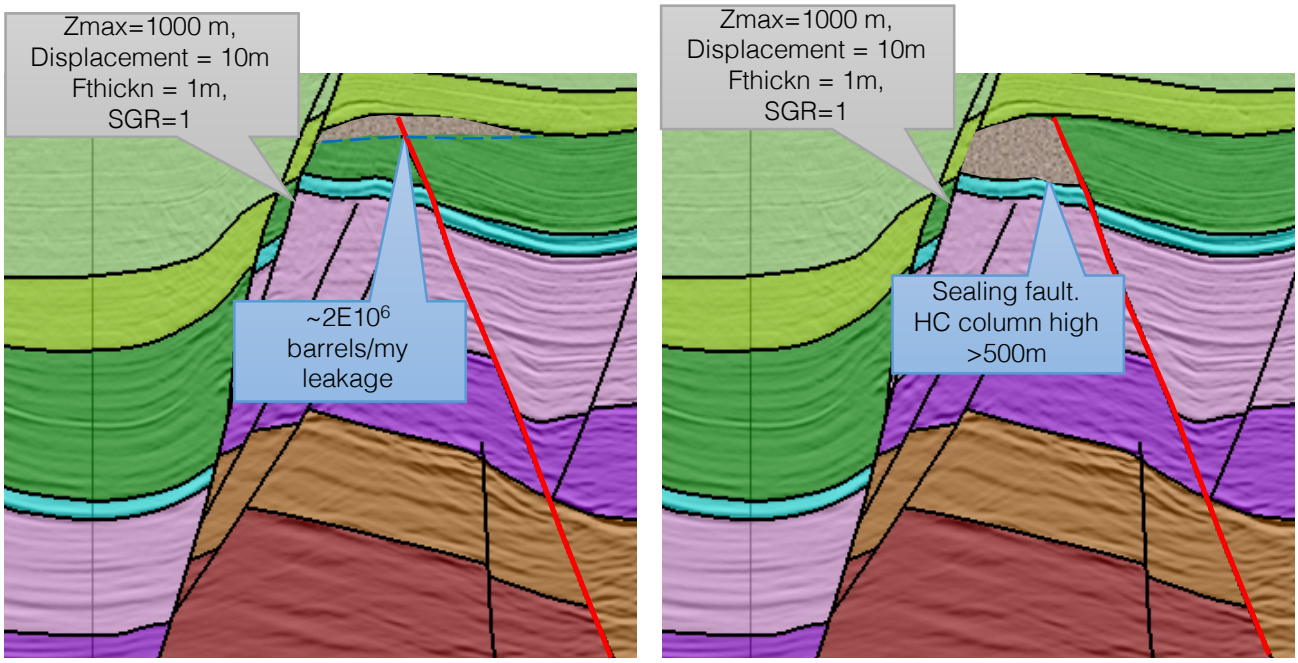


**Figure 3**. Sketch of the faulted trap showing two different exploration scenarios by migration algorithms of Darcy's flow (left panel) vs. Invasion Percolation (right panel).

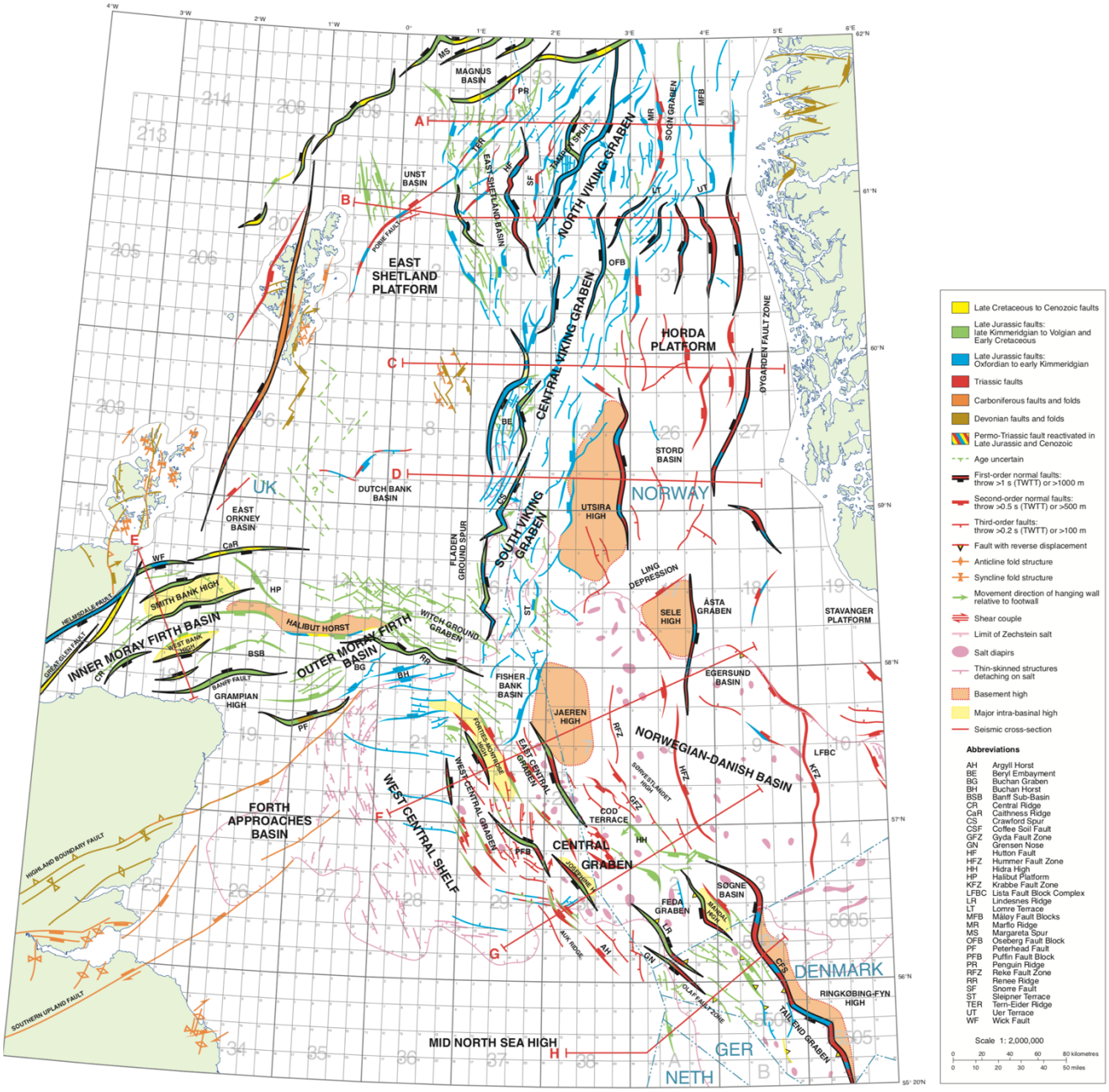


Figure 4. Tectonic map (Ahmadi et al., 2003) showing heavily faulted South Viking Graben area.

# SCIENTIFIC UNDERPINNING OF CONCEPTS OF GEOCHEMICAL INVERSION: DEVELOPING AND IMPROVING METHODS WITH APPLICATION TO PETROLEUM SYSTEM ANALYSIS

**Mei Mei[1,2], K.K. (Adry) Bissada[1], Thomas B. Malloy[1], L. Mike Darnell[1]**
[1]*Department of Earth and Atmospheric Sciences, University of Houston*
[2]*Department of Energy Resources Engineering, Stanford University*

## Abstract

Geochemical inversion is a process for inferring petroleum origin by the geochemical characteristics of the petroleum (Bissada et al., 1993). It is important for petroleum exploration and exploitation. However, routine approaches are burdened with numerous ambiguities and inconsistencies that require improvements (Peters et al., 2005; Wei et al., 2007; Bissada et al., 2016a,b). Here, an improved GC-MS/MS method was developed for simultaneous determination of saturate and aromatic biomarkers, diamondoids, and organo-sulfur compounds in the whole crudes. This method eliminates the need for group-type separation and avoids the loss of light-ends. The method was optimized, calibrated, and tested using diverse pure compounds and different types of crude oils. Comparison of the results indicates higher resolution, higher specificity, sensitivity, accuracy and precision for biomarker analysis. The newly developed analytical method, together with modified interpretation schemes, geological perspectives, and basin modeling were applied to unravel the origins of light crudes in the Almond Formation in southwestern Wyoming, USA (Fig. 1 and Fig. 2). The modified interpretation schemes entailed: (i) a basin-specific calibration of diamondoid-based thermal-maturity parameters; and (ii) modified $C_7$-hydrocarbon indices to infer source facies and thermal-maturity (Fig. 3 and Fig. 4). The comprehensive results suggest the petroleum in the Almond Formation originated from the downdip, highly mature (1.3 to 1.7% Ro) source rocks of the Lower Almond Formation/Upper Mesaverde Group in the Washakie and the Great Divide basins. Two papers based on our findings have been recently published on the Organic Geochemistry (M. Mei, et al, 2018a; 2018b).

## References

Bissada, K.K., Elrod, L.W., Robison, C.R., Darnell, L.M., Szymczyk, H.M., Trostle, J.L., 1993. Geochemical inversion – a modern approach to inferring source-rock identity from characteristics of accumulated oil and gas. Energy Exploration & Exploitation 11, 295–328.

Bissada, K. K., Tan, J. Q., Szymcyk, E. B., Darnell, L. M., Mei, M., 2016a. Group-type characterization of crude oil and bitumen. Part I: Enhanced separation and quantification of saturates, aromatics, resins and asphaltenes (SARA). Organic Geochemistry 95, 21-28.

Bissada, K. K., Tan, J. Q., Szymcyk, E. B., Darnell, L. M., Mei, M., 2016b. Group-type characterization of crude oil and bitumen. Part II: Efficient separation and quantification of normal-paraffins iso-paraffins and naphthenes (PIN). Fuel 173, 217-221.

Mei, M., Bissada, K. K., Malloy, T. B., Darnell, L. M., Liu, Z. F., 2018a. Origin of condensates and natural gases in the Almond Formation reservoirs in southwestern Wyoming, USA. Organic Geochemistry 124, 164-179.

Mei, M., Bissada, K. K., Malloy, T. B., Darnell, L. M., Liu, Z., Szymcyk, E. B., 2018b. Improved method for simultaneous determination of saturated and aromatic Biomarkers, organosulfur compounds and diamondoids in crude oils by GC-MS/MS. Organic Geochemistry 116, 35-50.

Peters, K.E., Walters, C.C., Moldowan, J.M., 2005. The Biomarker Guide. II. Biomarkers and Isotopes in Petroleum Systems and Earth History. Cambridge University Press, pp. 475–964.

Wei, Z.B., Moldowan, J.M., Zhang, S.C., Hill, R., Jarvie, D.M., Wang, H.T., Song, F.Q., Fago, F., 2007. Diamondoid hydrocarbons as a molecular proxy for thermal maturity and oil cracking: geochemical models from hydrous pyrolysis. Organic Geochemistry 38, 227–249.

**Figures**

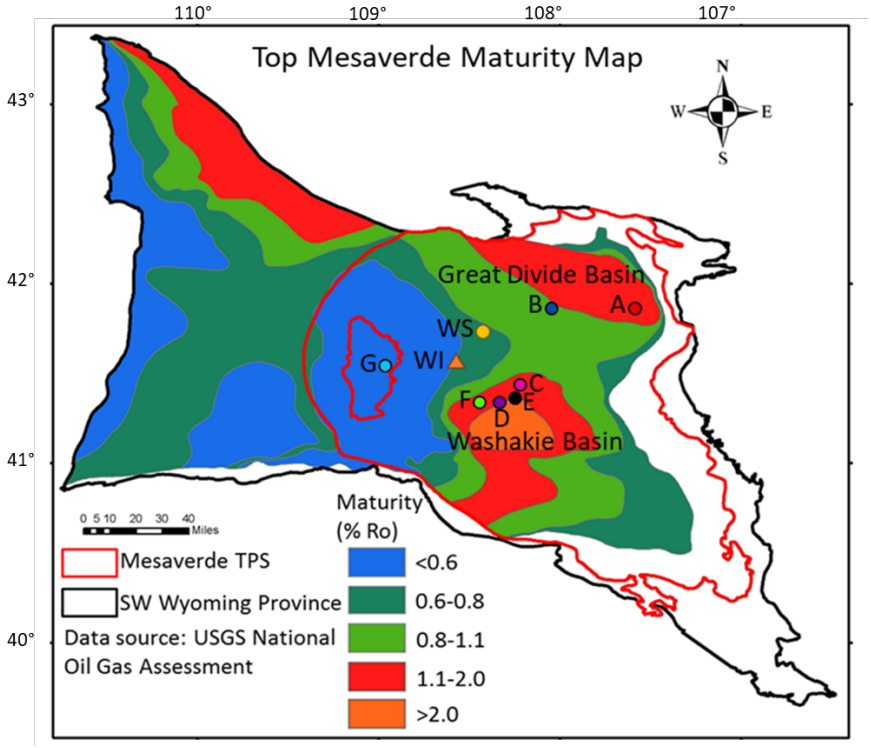


Fig. 1 Thermal maturity map for Top Mesaverde Group (modified from Johnson et al., 2005).

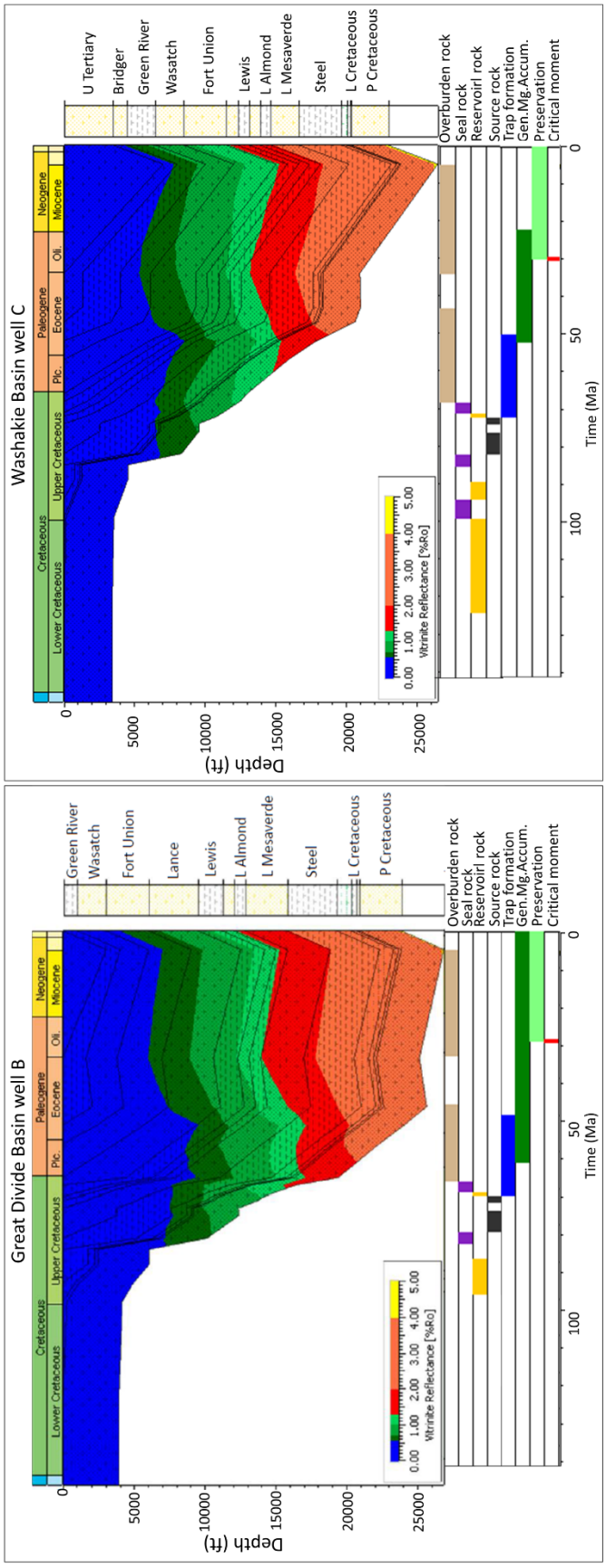


Fig. 2 Burial histories, thermal maturation histories and petroleum-system events charts for wells B and C in the Great Divide and Washakie basins, respectively.

Fig. 2 Burial histories, thermal maturation histories and petroleum-system events charts for wells B and C in the Great Divide and Washakie basins, respectively.

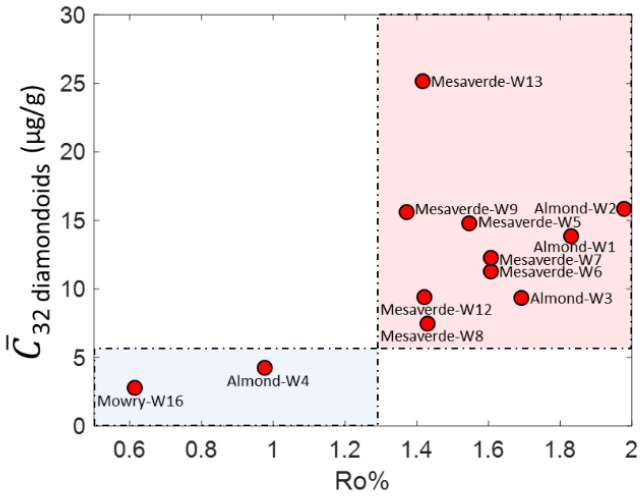


Fig. 3 Relation of vitrinite reflectance (Ro%) of Wyoming conventional core samples to the average concentration of 32 diamondoid compounds in the extractable organic matters (EOMs) of the same core samples. The corresponding rock data are shown in Table 1.

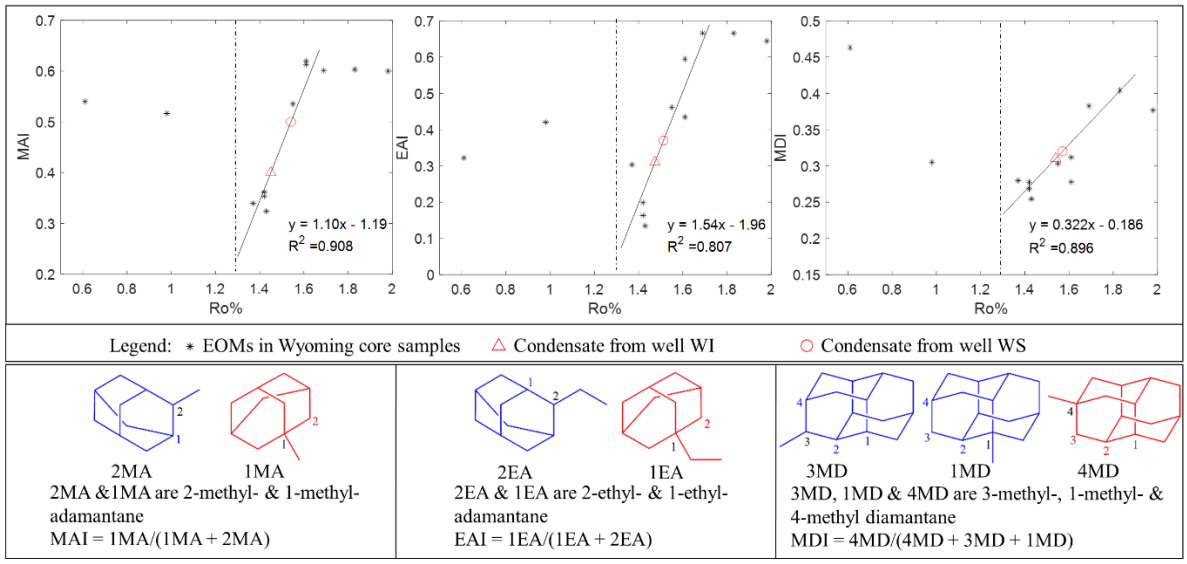


Fig. 4 Relations of vitrinite reflectance (Ro%) to diamondoid isomer ratios (MAI, EAI and MDI). Each linear regression equation and square of correlation coefficient R2 are computed for the samples with high-maturity (Ro 1.3%) along the regression fitting line.

# ANALYTICAL EQUATIONS FOR THE GORWTH OF CARBONATE PLATFORMS

**Nicolas Goudemand[1], Pulkit Singh[2], Jonathan Payne[2]**

[1]*Univ. Lyon, ENS de Lyon, CNRS, Univ. Claude Bernard Lyon 1, Institut de Génomique Fonctionnelle de Lyon, UMR 5242, 46 Allée d'Italie, F-69364 Lyon Cedex 07, France*

[2]*Department of Geological Sciences, Stanford University*

## Introduction

Carbonate platforms are unmatched repositories of our planet's physical, chemical and biological evolutionary history (Wilson 1975; Grotzinger 1986, 1989). Carbonate reservoirs are also host to more than 60% of world's oil and 40% of world's gas reserves (Roehl and Choquette,2012). One of the main challenges in understanding facies distribution in carbonate platforms is predicting the growth patterns of carbonate platforms through time. Predicting these growth patterns is essential in carbonate reservoir exploration as the growth patterns controls facies distribution and internal stratigraphic architecture of the carbonate platforms. Various forward stratigraphic modeling techniques have been used to simulate carbonate platform evolution as a function of sediment production, transport, tectonic subsidence, and eustasy. However, modeling the complex interaction between these physical factors generally leads to non-linear sets of equations that are not only inherently complex to solve but also prohibit the complete exploration of parameter space. To overcome this challenge, we have developed a comprehensive set of simple analytical equations with closed solutions that predict carbonate platform trajectories as function of initial platform height, subsidence, sediment production, transport, and eustasy.

## Methodology

Geometrically, an attached carbonate platform is distinguished by a flat inner platform abruptly transitioning into relatively steeper slope environment and into the adjacent basin (Figure 1). The platform geometries are categorized as prograding, aggrading or retrograding based on the changing position of the platform margin through time (Read 1982). We have assumed an initial platform geometry and using simple assumptions about subsidence, sediment production and transport we were able to develop analytical equations which can predict the evolution of platform geometries and precisely quantify the controlling factors like sediment production rate on the platform top and the width of the margin contributing to the growth of platform.

## Results and Conclusions

In summary, the model predicts the conditions under which platforms will prograde, aggrade, or retrograde and how slope geometry impacts these tendencies. To test the practical applicability of our growth equations, we applied our model to the Permian Capitan Reef of West Texas and Carboniferous Sierra Del Cuera carbonate platform in Spain. Our models can reliably predict the growth trajectories of carbonate platform margins using the simple assumptions about subsidence, pelagic sedimentation, sediment

production and transport. These models can be used as effective exploration tools because they can extract useful information about physical factors constraining the carbonate platform evolution with limited information.

**References**

Grotzinger, J.P., 1986. Cyclicity and paleoenvironmental dynamics, Rocknest platform, northwest Canada. *Geological Society of America Bulletin*, *97*(10), pp.1208-1231.

Grotzinger, J.P., 1989. Facies and evolution of Precambrian carbonate depositional systems: emergence of the modern platform archetype.

Read, J.F., 1982, Carbonate platforms of passive (extensional) continental margins: types, characteristics and evolution: *Tectonophysics*, v. 81, p. 195-212

Roehl, P.O. and Choquette, P.W. eds., 2012. *Carbonate petroleum reservoirs*. Springer Science & Business Media.

Wilson, J.L., l., 1975, Carbonate facies in geologic history.

Figures:

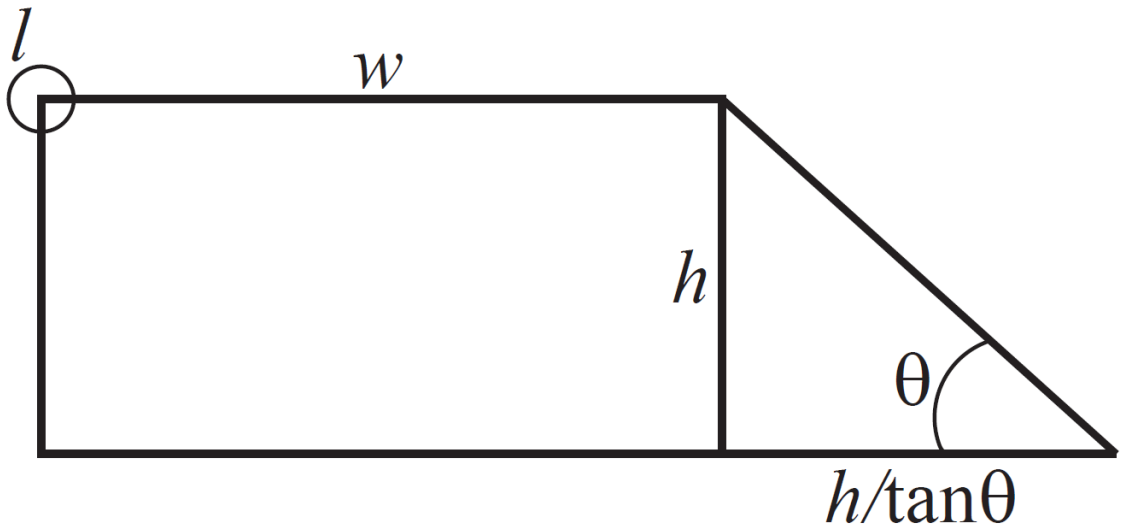


Fig 1. The initial platform geometry assumed for carbonate platform.

# INTERACTIONS BETWEEN SEDIMENT PRODUCTION AND TRANSPORT IN THE DEVELOPMENT OF CARBONATE PLATFORMS: A CASE STUDY FROM THE GREAT BANK OF GUIZHOU, SOUTH CHINA

**Xiaowei Li[1] and Jonathan L. Payne[1]**
[1]*Department of Geological Sciences, Stanford University, geo.xwli@gmail.com*

## Introduction

Carbonate platforms are valuable archives of ancient environmental changes and hold more than half of the world's oil reserves. However, the physical, chemical, and biological processes by which they develop remain incompletely understood. A significant challenge remains in quantitatively assessing the relative contributions of sediment production and subsequent transport in generating platforms with significant variation in overall geometry through time.

## Methodology

Stratigraphic forward modeling (DIONISOS) is used to (1) mimic the geometry of a real isolated carbonate platform of Permian-Triassic age that exhibits variation in geometry across time and (2) quantify the relative roles of sediment production and transport in controlling the evolution of platform geometry.

## Basin model and results

Model results show that the geometry of the platform is most sensitive to sediment transport, moderately sensitive to maximum carbonate production rate, and least sensitive to productivity-depth curve. The ramp-to-shelf transition of the platform during Early Triassic time, which occurred without microbial and skeletal reef builders at the margin, can be explained by other factors so long as they limited sediment transport from shallow water areas of high production to accommodation space in the adjacent basin. In this particular case, an extremely high carbonate saturation state of tropical seawater ($\Omega$~10), which is much greater than that of modern tropical seawater ($\Omega$~5) may have caused early lithification of ooid shoals on the platform margin, inhibiting sediment transport into the basin. The model results also suggest that carbonate platforms can still prograde basinward with very low transport rate when sediment production occurs on the slope through an oligophotic factory.

## Summary and Conclusions

The efficiency with high carbonate saturation state or high potential rates of biological sediment production are turned into real sediment accumulation and platform growth is influenced by sediment transport. Results from these model simulations suggest that steep-sided carbonate platforms lacking slope factories that extend hundreds of meters below sea-level are often transport-limited rather than production-limited.

# SCALING ANALYSIS OF THE COUPLED COMPACTION, KEROGEN CONVERSION, AND PETROLEUM EXPULSION DURING GEOLOGICAL MATURATION

**Qingwang (Kevin) Yuan[1], Yashar Mehmani[1], Alan Burnham[1], Alexandre Lapene[2], Johannes Wendebourg[2], Hamdi Tchelepi[1]**
[1]*Department of Energy Resources Engineering, Stanford University*
[2]*TOTAL E&P Research & Technology USA*

## Introduction

Porosity rebound is associated with the kerogen conversion into hydrocarbons and the overpressure development in the coupled sedimentary compaction, kerogen conversion, sorption, and fluids expulsion processes (Luo and Vasseur, 1996; Swarbrick et al., 2002). There are a large number of variables with uncertainties in the coupled processes. Uncertainty analysis to determine their sensitivity and importance with fully nonlinear 3D basin-scale numerical simulation is very time-consuming (Wolf et al., 2012). Moreover, typical uncertainty analysis by varying each variable while fixing others is only based on the typical base case. Considering the nonlinear behavior of the response in terms of the input parameters, this uncertainty analysis is limited and may not be able to fully represent the relative importance of parameters with uncertainties (Hicks Jr. et al., 2012). To perform uncertainty analysis with numerous parameters in a more comprehensive way in the coupled processes during maturation, the scaling analysis was performed, which is simpler and more efficient to determine the relative importance of different mechanisms.

## Methodology

The scaling analysis was conducted as follows. First, a unit cell model for the volume fraction change of each component and porosity was developed. Elastic and inelastic deformation of solid phases, thermal expansion, primary and secondary cracking, sorption of hydrocarbons, and expulsion were taken into account. The schematic for this model is shown in Figure 1. Through inspectional analysis method, the dimensionless equations as well as a group of dimensionless numbers are obtained. Then, the two-level experimental design was used to generate the minimum number of combinations and corresponding scenarios which we solved with our self-developed simulator. The relative importance of the dimensionless numbers and their corresponding mechanisms are determined and ranked by the normalized coefficients. The results are compared with those from 1D modeling using PetroMod.

## Results

Through scaling analysis, the corresponding dimensionless numbers for the competing mechanisms of compaction, heating, reaction, expulsion, and hydrocarbon sorption are identified. We reduced the influencing factors from 53 physical parameters to 43 dimensionless numbers, 5 of which are much more important than others for porosity rebound (Figure 2). The ranking of the most important mechanisms associated with the dimensionless numbers are: initial kerogen content, geothermal heating, compaction coefficient, fluid expulsion, and reaction during hydrocarbon generation. For

overpressure, the same most important dimensionless numbers are also involved. The results are comparable with those from PetroMod simulations, with just minor differences in the ranking of the most important dimensionless numbers, as shown in Figures 2 and 3.

## Conclusions

The competing mechanisms during porosity rebound and overpressure development in the coupled processes are identified and represented by a group of dimensionless numbers. Our self-developed model can determine the relative importance of them. The results are consistent with those using PetroMod, but our model is simpler and more efficient in uncertainty analysis for basin modeling.

## References

Luo, X. and Vasseur, G., 1996, Geopressuring mechanism of organic matter cracking: Numerical modeling: AAPG, v. 80, p. 856-874.

Swarbrick, R.E., Osborne, M.J., and Yardley, G.S., 2002, Comparison of overpressure magnitude resulting from the main generating mechanisms: AAPG Memoirs, v. 76, p. 1–12.

Wolf, S., Faille, I., Pegaz-Fiornet, S., Willien, F., and Carpentier, B., A new efficient scheme to model hydrocarbon migration at basin scale: A pressure-saturation splitting, in K. E. Peters, D. J. Curry, and M. Kacewicz, eds., New horizons in research and applications, AAPG Hedberg Series, p. 197-205.

Hicks Jr., P. J., Hardy, M. J., Shosa, J. D., and Townsley, M. B., Identifying and quantifying significant uncertainties in basin modeling, in K. E. Peters, D. J. Curry, and M. Kacewicz, eds., New horizons in research and applications, AAPG Hedberg Series, p. 207-219.

**Figures:**

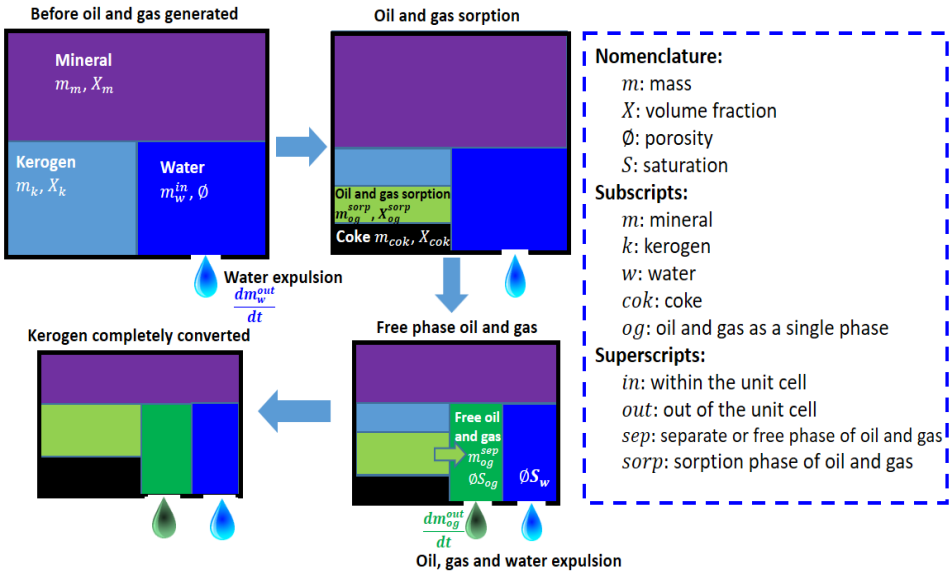


Figure 1. Unit cell model for the coupled proceses of compaction, kerogen conversion, sorption, and fluid expulsion.

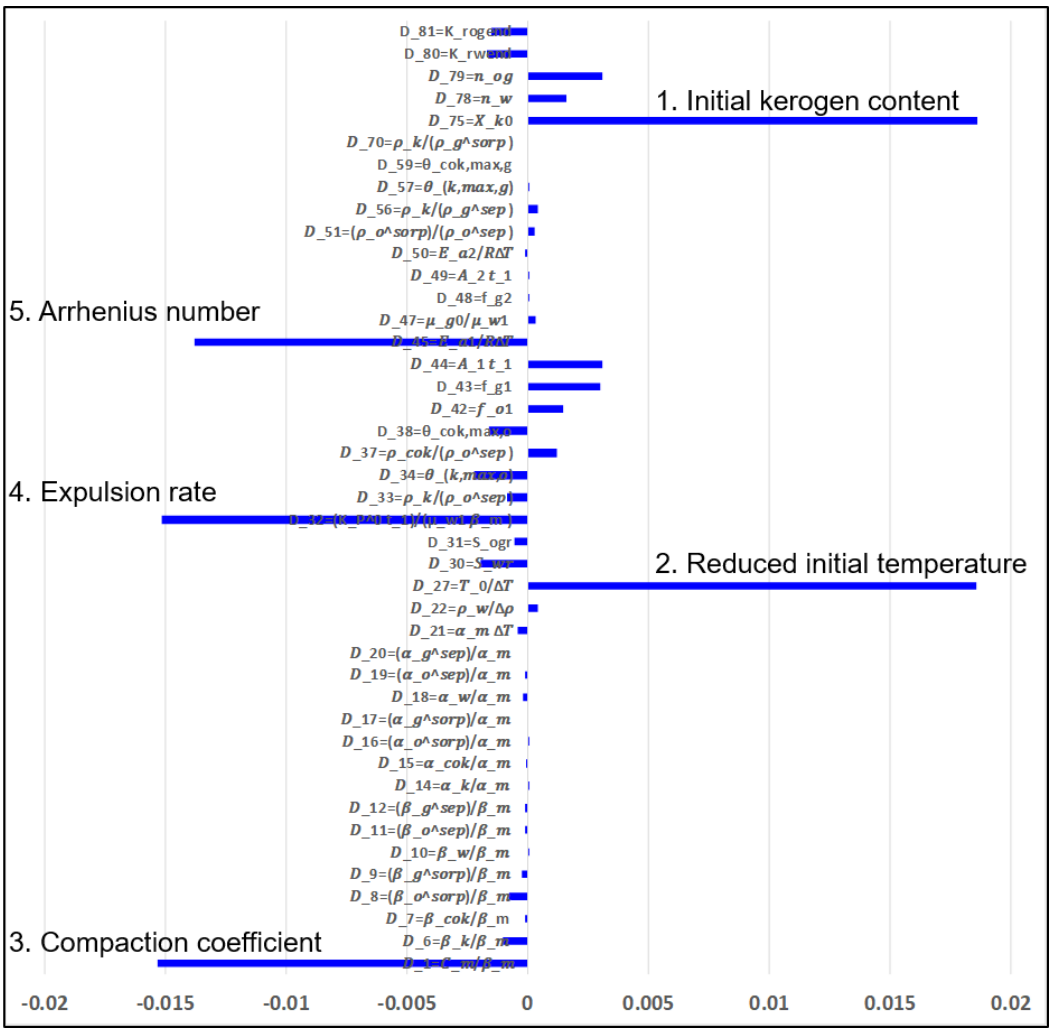


Figure 2. Relative importance of dimensionless numbers from our model (The ranking of importance is initial kerogen content, reduced initial temperature, compaction coefficient, expulsion rate, and Arrhenius number).

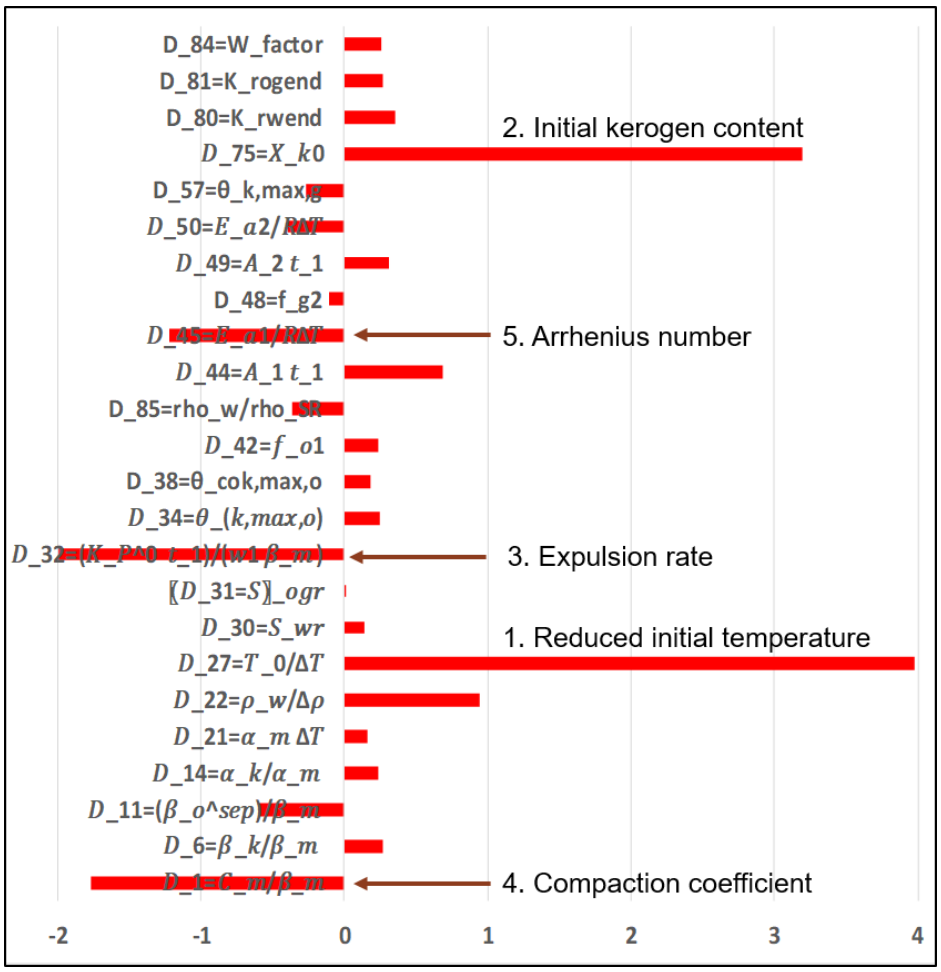

Figure 3. Relative importance of dimensionless numbers/mechanisms from PetroMod 1D results (The ranking of importance is reduced initial temperature, initial kerogen content, expulsion rate, compaction coefficient, and Arrhenius number).